PROGRESS REPORT

ON

CORRELATION OF LABORATORY TESTS WITH FULL SCALE SHIP PLATE FRACTURE TESTS

BY

C. WAGNER AND E. P. KLIER

Pennsylvania State College
Under Bureau of Ships Contract NObs-31217

COMMITTEE ON SHIP CONSTRUCTION

DIVISION OF ENGINEERING AND INDUSTRIAL RESEARCH

NATIONAL RESEARCH COUNCIL

ADVISORY TO

SHIP STRUCTURE COMMITTEE

UNDER

Bureau of Ships, Navy Department
Contract NObs-34231

SERIAL NO. SSC-18

COPY NO.............

DATE: MAY 12, 1948

NATIONAL RESEARCH COUNCIL
Washington 25, D. C.

May 12, 1948

Chief, Bureau of Ships
Navy Department
Washington 25, D. C.

Dear Sir:

Attached is Report Serial No. SSC-18 entitled "Correlation of Laboratory Tests with Full Scale Ship Plate Fracture Tests." This report has been submitted by the contractor as a progress report of the work done on Research Project SR-96 under Contract NObs-31217 between the Bureau of Ships, Navy Department and the Pennsylvania State College.

The report has been reviewed and acceptance recommended by representatives of the Committee on Ship Construction, Division of Engineering and Industrial Research, NRC, in accordance with the terms of the contract between the Bureau of Ships, Navy Department and the National Academy of Sciences.

Very truly yours,

Frederick M. Feiker

Frederick M. Feiker, Chairman
Division of Engineering and
Industrial Research

Enclosure

Preface

The Navy Department through the Bureau of Ships is distributing this report to those agencies and individuals who were actively associated with the research work. This report represents a part of the research work contracted for under the section of the Navy's directive "to investigate the design and construction of welded steel merchant vessels."

The distribution of this report is as follows:

Copy No. 1 - Chief, Bureau of Ships, Navy Department
Copy No. 2 - Dr. D. W. Bronk, Chairman, National Research Council

Committee on Ship Construction

Copy No. 3 - V. H. Schnee, Chairman
Copy No. 4 - J. L. Bates
Copy No. 5 - H. C. Boardman
Copy No. 6 - Paul Ffield
Copy No. 7 - M. A. Grossman
Copy No. 8 - C. H. Herty, Jr.
Copy No. 9 - A. B. Kinzel
Copy No. 10 - J. M. Lessells
Copy No. 11 - G. S. Mikhalapov
Copy No. 12 - J. Ormondroyd
Copy No. 13 - H. W. Pierce
Copy No. 14 - E. C. Smith
Copy No. 15 - T. T. Watson
Copy No. 16 - Finn Jonassen, Research Coordinator

Members of Project Advisory Committees SR-25, SR-87, SR-92, SR-96, SR-97, SR-98, SR-99 and SR-100

Copy No. 16 - Finn Jonassen, Chairman
Copy No. 17 - R. H. Aborn
Copy No. 18 - L. C. Bibber
Copy No. 5 - H. C. Boardman
Copy No. 6 - Paul Ffield
Copy No. 7 - M. A. Grossman
Copy No. 8 - C. H. Herty, Jr.
Copy No. 19 - C. E. Jackson
Copy No. 20 - C. H. Jennings
Copy No. 10 - J. M. Lessells
Copy No. 11 - G.S. Mikhalapov
Copy No. 12 - J. Ormondroyd
Copy No. 13 - H. W. Pierce
Copy No. 14 - E. C. Smith
Copy No. 15 - T. T. Watson
Copy No. 21 - A. G. Bissell, Bureau of Ships, Liaison
Copy No. 22 - Mathew Letich, American Bureau of Shipping, Liaison
Copy No. 23 - James McIntosh, U. S. Coast Guard, Liaison
Copy No. 24 - Capt. F. W. Myers, Jr., Transportation Corps Board, Liaison
Copy No. 25 - E. Rassman, Bureau of Ships, Liaison
Copy No. 26 - Comdr. R. D. Schmidtman, U. S. Coast Guard, Liaison

Copy No. 27 - T. L. Soo-Hoo, Bureau of Ships, Liaison
Copy No. 28 - Wm. Spraragen, Welding Research Council, Liaison
Copy No. 29 - R. E. Wiley, Bureau of Ships, Liaison
Copy No. 30 - J. L. Wilson, American Bureau of Shipping, Liaison

Ship Structure Committee

Copy No. 31 - Rear Admiral Ellis Reed-Hill, USCG, Chairman
Copy No. 32 - Rear Admiral Charles D. Wheelock, USN, Bureau of Ships
Copy No. 33 - Brigadier General Paul F. Yount, War Department
Copy No. 4 - J. L. Bates, U. S. Maritime Commission
Copy No. 34 - D. P. Brown, American Bureau of Shipping
Copy No. 3 - V. H. Schnee, Committee on Ship Construction, Liaison

Ship Structure Subcommittee

Copy No. 35 - Captain L. V. Honsinger, USN, Bureau of Ships, Chairman
Copy No. 36 - Captain R. A. Hinners, USN, David Taylor Model Basin
Copy No. 37 - Comdr. R. H. Lambert, USN, Bureau of Ships
Copy No. 26 - Comdr. R. D. Schmidtman, USCG, U. S. Coast Guard Headquarters
Copy No. 24 - Capt. F. W. Myers, Jr., Transportation Corps Board, U. S. Army
Copy No. 38 - Hubert Kempel, Office Chief of Transportation, War Department
Copy No. 22 - Mathew Letich, American Bureau of Shipping
Copy No. 39 - R. M. Robertson, Office of Naval Research, U. S. Navy
Copy No. 40 - I. J. Wanless, U. S. Maritime Commission
Copy No. 29 - R. E. Wiley, Bureau of Ships, U. S. Navy
Copy No. 30 - J. L. Wilson, American Bureau of Shipping
Copy No. 16 - Finn Jonassen, Liaison Representative, NRC
Copy No. 41 - E. H. Davidson, Liaison Representative, AISI
Copy No. 42 - Paul Gerhart, Liaison Representative, AISI
Copy No. 28 - Wm. Spraragen, Liaison Representative, WRC

Navy Department

Copy No. 43 - Comdr. R. S. Mandelkorn, USN, Naval Administrative Unit
Copy No. 21 - A. G. Bissell, Bureau of Ships
Copy No. 44 - J. W. Jenkins, Bureau of Ships
Copy No. 45 - Noah Kahn, New York Naval Shipyard
Copy No. 46 - I. R. Kramer, Office of Naval Research
Copy No. 47 - W. R. Osgood, David Taylor Model Basin
Copy No. 48 - N. E. Promisel, Bureau of Aeronautics
Copy No. 49 - K. D. Williams, Bureau of Ships
Copy No. 50 - Naval Academy, Post Graduate School
Copy No. 51 - Naval Research Laboratory
Copies 52 and 53 - U. S. Naval Engineering Experiment Station
Copy No. 54 - New York Naval Shipyard, Material Laboratory
Copy No. 55 - Industrial Testing Laboratory, Philadelphia Naval Shipyard
Copy No. 56 - Philadelphia Naval Shipyard
Copies 57 and 58 - Publications Board, Navy Dept. via Bureau of Ships, Code 330c
Copies 59 and 60 - Technical Library, Bureau of Ships, Code 337-L

U. S. Coast Guard

Copy No. 61 - Captain R. B. Lank, Jr., USCG
Copy No. 62 - Captain G. A. Tyler, USCG
Copy No. 63 - Testing and Development Division

U. S. Maritime Commission

Copy No. 64 - E. E. Martinsky

Representatives of American Iron and Steel Institute
Committee on Manufacturing Problems

Copy No. 65 - C. M. Parker, Secretary, General Technical Committee, American Iron and Steel Institute
Copy No. 18 - L. C. Bibber, Carnegie-Illinois Steel Corporation
Copy No. 8 - C. H. Herty, Jr., Bethlehem Steel Company
Copy No. 14 - E. C. Smith, Republic Steel Company

Welding Research Council

Copy No. 66 - C. A. Adams
Copy No. 67 - Everett Chapman
Copy No. 68 - LaMotte Grover
Copy No. 28 - Wm. Spraragen

Copy No. 69 - F. M. Feiker, Chairman, Div. Engineering & Industrial Research, NRC
Copy No. 3 - V. H. Schnee, Chairman, Committee on Ship Construction
Copy No. 16 - Finn Jonassen, Research Coordinator, Committee on Ship Construction
Copy No. 70 - C. Wagner, Investigator, Research Project SR-96
Copy No. 71 - E. P. Klier, Investigator, Research Project SR-96
Copy No. 72 - A. Boodberg, Investigator, Research Project SR-92
Copy No. 10 - J. M. Lessells, Investigator, Research Project SR-101
Copy No. 73 - Scott B. Lilly, Investigator, Research Project SR-98
Copy No. 74 - C. H. Lorig, Investigator, Research Project SR-97
Copy No. 75 - J. R. Low, Jr., Investigator, Research Project SR-96
Copy No. 76 - C. W. MacGregor, Investigator, Research Project SR-102
Copy No. 77 - Albert Muller, Investigator, Research Project SR-25
Copy No. 78 - E. R. Parker, Investigator, Research Project SR-92
Copy No. 79 - Geo. Sachs, Investigator, Research Project SR-99
Copy No. 80 - C. E. Sims, Investigator, Research Project SR-87
Copy No. 81 - C. B. Voldrich, Investigator, Research Project SR-100
Copy No. 82 - Clarence Altenburger, Great Lakes Steel Company
Copy No. 83 - A. B. Bagsar, Sun Oil Company
Copy No. 84 - E. L. Cochrane, Massachusetts Institute of Technology
Copy No. 85 - George Ellinger, National Bureau of Standards
Copy No. 86 - M. Gensamer, Carnegie-Illinois Steel Company
Copy No. 87 - O. J. Horger, Timken Roller Bearing Company
Copy No. 88 - S. L. Hoyt, Battelle Memorial Institute
Copy No. 89 - Bruce Johnston, Fritz Laboratory, Lehigh University
Copy No. 90 - E. M. MacCutcheon, Jr., David Taylor Model Basin
Copy No. 91 - N. M. Newmark, University of Illinois
Copy No. 92 - L. J. Rohl, Carnegie-Illinois Steel Corp.
Copy No. 93 - W. P. Roop, Swarthmore College
Copy No. 94 - Saylor Snyder, Carnegie-Illinois Steel Corp.
Copy No. 95 - John Vasta, Code 442, Bureau of Ships, Navy Department
Copies 96 thru 120 - Charles Wright, British Joint Services Mission (Navy Staff)
Copy No. 121 - Carl A. Zapffe, Carl A. Zapffe Laboratories
Copy No. 122 - International Nickel Co., Inc., Attn. T. N. Armstrong
Copy No. 123 - Transportation Corps Board, Brooklyn, N. Y.

Copies 124 thru 128 - Library of Congress via Bureau of Ships, Code 330c
Copy No. 129 - File Copy, Committee on Ship Construction
Copy No. 130 - NACA, Attn: Materials Research Coordination, U. S. Navy

Copies 131 thru 135 - Bureau of Ships

Copy No. 136 -
Copy No. 137 - Case Institute of Technology, Cleveland, Ohio: 9/29/48
Copy No. 138 -
Copy No. 139 - Miss Marian Sandomire, BuShips, 7/26/49
Copy No. 140 - C. Robert Riccio, CSS, 8/12/49
Copy No. 141 - J. E. McMurtt - 2/1/50
Copy No. 142 - Capt. W. P. Roop - 8/14/50
Copy No. 143 - [illegible]
Copy No. 144 - J. F. MILLAN, Caterpillar Tractor Co. 11-24-52
Copy No. 145 - T. Akagawa, K - Japan - 12-28-53
Copy No. 146 -
Copy No. 147 -
Copy No. 148 -
Copy No. 149 -
Copy No. 150 -

(Total - 150 copies)

NAS-NRC (Library) 8/10/56 - 1 copy
Mr. J. C. Mackie, Sydney, Nova Scotia, 1 copy - 9/25/56

PROGRESS REPORT

Navy Bureau of Ships, Contract NObs-31217
Project SR-96

CORRELATION OF LABORATORY TESTS WITH FULL SCALE SHIP PLATE FRACTURE TESTS

Date: January 3, 1948

By: C. Wagner
E. P. Klier

MINERAL INDUSTRIES EXPERIMENT STATION
SCHOOL OF MINERAL INDUSTRIES
THE PENNSYLVANIA STATE COLLEGE
STATE COLLEGE, PENNSYLVANIA

TABLE OF CONTENTS

LIST OF TABLES

LIST OF FIGURES

Navy Contract NObs-31217

Research Project SR-96

CORRELATION OF LABORATORY TESTS WITH FULL SCALE SHIP PLATE FRACTURE TESTS

Introduction

In the investigation of the possible development of a laboratory test for correlation with large plate notched tension tests on ship quality plate, a series of notch bend tests has been conducted. It was expected that an adequate laboratory test would display the same transition temperature or one that was readily adjustable to that observed for the large plate tensions tests conducted at the Universities of Illinois and California.[1,2]

Initially, standard Charpy impact tests were made on all of the steels[3] and the results compared with those for the 72" wide plate tests. The comparisons showed that no direct correlation existed between these two widely differing types of notched specimen tests.

One of the striking inadequacies of the impact test was the failure to show a difference between steels A and C, a difference which was most pronounced in the 72" wide plate tests. Separation of steels A and C to some extent, and in the right direction, was achieved by the use of prestrained Charpy keyhole-notch test bars, but the overall results did not warrant the further use of this test, as the temperatures of tough to brittle transition were too low to use direct correlation procedures. Because of this, a program was initiated in which the effects of speci-

---

1,2,3 - See Bibliography

men size, geometry, and testing velocity on the temperature of transition from tough to brittle behavior were investigated.

The results of slow bend testing (at 1" per minute) of standard V-notch Charpy impact bars did not separate Steels A and C. The transition temperatures for these two steels were appreciably lowered however, as compared to those obtained from the impact test, and fell in the range of temperatures observed for the large plate test results. An increase in the specimen size to 0.788" high x .394" wide gave transition temperatures for most of the steels tested which were 10° to 20°F below those for the 72" wide plate tests.

Finally, specimens were prepared which were full plate thickness in width and 0.788" in height. The tough to brittle transition, as measured by energy absorption values, occurred for these specimens at temperatures which agreed fairly well with the transition ranges for the 72" wide plates.[4]

Specimens of this type, when tested across a 40 millimeter span, had the disadvantage of not breaking completely. By drilling the compression zone from the specimen and using a hardened steel pin on which to apply the load, as described by Schnadt[5], it was possible to circumvent this difficulty.

The present report is confined to the outline of experiments with this "Schnadt type" specimen and the results pertaining to those experiments.

The personnel contributing to the collection of these data are as follows:

J. R. Low, Jr. - Technical Representative

M. Gensamer - Technical Advisor

F. C. Wagner - Supervisor

E. P. Klier - Investigator

Eunice Marks - Research Assistant

M. A. Biship - Research Assistant

Mina Moessen - Technical Labor

Herman Colyer - Technical Labor

Philip Vonada - Technical Labor

Eleanor Tevlin - Drafting

Steels

The steels are those used formerly and are designated in the same manner.[3]

Testing Program

Tests were first conducted on certain sections from 72" wide flat plate tests in order to check previous results obtained for undrilled specimens.

Further tests were then conducted on material from all of the project steels, using both LH and BH orientations. The meanings of the designations LH and BH are as shown in Figure 51; L, H. and B represent directions in the plate parallel to the length (taken as the rolling direction), the height or thickness, and breadth, respectively. The first letter in the designation of the specimen indicates the direction of the long axis of the specimen, while the second letter indicates the direction of the notch. For example, an LH specimen is one with the specimen axis in the rolling direction and the notch in the thickness direction.

Specimen Preparation

Specimens for this set of experiments were prepared in the following manner:

Bars which were about $2\frac{1}{4}$" in width were sawed from the plate and machined by shaping to 2.16", this latter dimension being the final length of the test bars. These bars were then sawed transversely into bars slightly larger than test specimen height, and again machined by shaping on two sides to 0.788". This procedure gave test specimens of 0.788" in height, full plate thickness in width, and 2.16" in length. The standard V-notch (.079" depth, 0.01" radius, 45° included angle) was used. After notching, the specimens were placed in a drilling jig so set up that a $\frac{1}{2}$" diameter hole could be drilled back of the notch. The distance from the base of the notch to the edge of the hole was held at 0.312". Figure 1 is a photograph of the test specimen, while Figure 3 is a line drawing giving the dimensions of this specimen.

Testing Equipment

No changes were necessary in equipment from that used previously[4] for conducting the slow bend notched-bar test with the exception of the hardened steel pins on which the load was applied. The photograph, Figure 2, shows the equipment as assembled before the testing operation, while Figure 4 shows the bending fixture with a notched bar in place. This fixture has a 40 mm breaking span, with a centering device being used against the back and one end of the specimen. According to whether the desired testing temperature was above or below the freezing point of water, water or acetone was used as the temperature control medium.

Testing Procedure

The first step in testing is the adjustment of the temperature of the bath to the desired value.

For temperatures between 60°F and 140°F, tap water is used, being mixed in the required proportions at the faucets and piped to the container. For temperatures from 32°F to 60°F, ice is used to cool water as required. Finally, for temperatures below 32°F, acetone is cooled with dry ice to the proper temperature range.

After the desired bath temperature is reached, a holding period of at least 10 minutes is allowed to be certain that the bending fixture attains the bath temperature. Specimens are then immersed in the bath and held for a minimum of 4 minutes before breaking. As shown by the cooling curve in Figure 47 which was determined by means of a thermocouple inserted in a small hole drilled in the side of the specimen just above the notch, this length of time is adequate for the small mass of the slow bend notched-bar test specimen.

The specimen is then centered on the anvils by means of a stop which places the notch in the middle of the 40 mm. breaking span and immediately under the punch which applies the load.

The centering device is then removed and the specimen is bent to fracture at a deflection rate of about one inch per minute. After fracture, the specimen is removed from the bath, dried, and examined for data on deformation and fracture characteristics.

Representation of Test Data

In conducting a slow notch-bend test using the Schnadt specimen, two observations are made, both after the broken specimen is removed from the testing fixture. First the fracture surface is examined and the percent of the fracture surface which has a ductile (fibrous) appearance is estimated. Second, the width of the fracture at the surface of the drilled hole is measured by means of a point micrometer. This width (w_1) together with the original width (w_o) at the same point is used to compute the contraction $w_o - w_1$ which is taken as a measure of the energy absorbed in fracturing the metal just below the notch.

The transition temperature can be determined in two ways: namely, from fracture characteristics or from lateral contraction at the fracture edge. The transition temperatures obtained by either of these methods are in satisfactory agreement with each other and with 72" wide plate test results.

Some discussion of the reasons for using the lateral contraction measurements rather than total energy absorption values is in order. In comparing load deflection curves for Schnadt type specimens corresponding to ductile and brittle failures, it was found that there was very little difference in total energy absorption as determined by the wedge extensometer method. As is shown by the curves in Figure 48 the energy absorption values as represented by the area under the load-deflection diagrams are, in this case, too nearly identical for convenient use in plotting energy absorption versus temperature curves. The energy determined from the load-deflection curves is a total energy which includes the energy of deformation of the specimen at the supports. Since this latter energy represents a large fraction of the total, particularly in a ductile specimen, the behavior of the metal just below the notch is obscured in the load-deflection curves.

Since deformation in the cross-section containing the notch is an indication of the energy absorption of the volume of metal beneath the notch, it is considered a valid procedure to substitute the change in width measurements for total energy absorption values. This is particularly true for the Schnadt type specimen because of the removal of the compression zone, and because of the localized deformation due to the V-notch. After obtaining values of $w_o - w_1$ and percent ductile fracture for any particular set of specimens, the data are plotted on graphs with $w_o - w_1$ or percent ductile fracture as the ordinates and temperature of testing as the abscissas. The way in which the curves are drawn on the graphs is dependent on the degree of scatter. In cases where the data show negligible scatter, a single curve is drawn by visual estimate, and the transition temperature is taken as the point on the curve which corresponds to the midpoint between the upper and lower portions of the curve. However, in cases where scatter exists, scatter bands are indicated on the curves and the transition temperature is indicated as the approximate mean of this range. The summary graphs shown are all drawn as single curves to simplify the representation.

Results of Slow Bend Testing

The fracture type vs. temperature curves are presented in Figures 15 to 24 and 36 to 46, and the curves of $w_o - w_1$ vs. temperature are shown in Figures 5 to 14, and 25 to 35. The results for both types of curves are summarized in Table I, where it is shown that good agreement exists in a majority of cases.

There are exceptions however, in the case of the Br and H steels particularly. The low transition temperature values for these steels appear to be a function of extreme "fissuring" in the bars. This longitudinal splitting of the bars has the effect of relieving the transverse stress component and hence, lowering the transition temperature to an extent which is presumably dependent on the number and size of fissures present. Experimental confirmation of this phenomenon was obtained for the Br steel by comparison of two sets of data. One of these sets, which was taken from the 72" wide flat plate specimen, B1A, showed no fissuring and gave a transition temperature of about 25°F, while a set taken from virgin plate manifested fissuring and indicated a transition temperature of -25°F. Curves are shown in Figure 49 for $w_o - w_1$ versus temperature which illustrates this and the photograph in Figure 50 shows the difference in fissuring.

Table II shows the estimated transition temperatures on the basis of $w_o - w_1$ values for specimens taken from several additional large plate test specimen sections.

Photographs of the LH orientation specimens of E and Br steels are shown in Figures 52a,-b,-c and 53a,-b,-c respectively. In the photographs of the E steel specimens, it can be seen that there are only three specimens which are not consistent with the general behavior; these are, one ductile fracture at 80°F, one ductile fracture at 75°F, and one partly ductile fracture at 60°F. In the fracture surface of each of these three specimens some fissuring is evident, with the specimen at 60°F being particularly interesting as it shows the remarkable effect of one large fissure on a specimen about 25°F below the transition temperature.

The fracture surfaces of all ductile specimens of Br steel show fissuring to a large extent. The fissures are small, ranging in length from a maximum of 3 mm. downward.

In the previous report on this subject[4], it was indicated that changing the orientation of the specimen had some effect on raising the transition temperature for steels Br and H. The entire set of project steels was tested in BH orientation, and the indications now are that this method is not effective in eliminating the effects of fissuring, as shown in Table I.

In Table A-I of the appendix, all of the data used in drawing the curves in Figures 5 to 46 are tabulated.

Conclusions

It is evident from the foregoing data that the Schnadt type slow bend test is an adequate test to reveal the large plate fracture characteristics of the project steels so long as fissuring transverse to the notch does not occur. When such fissuring occurs, the transition temperature is markedly lower than that reported for the 72" wide internally notched plate. However, such fissuring is readily evident so should not impair the satisfactory application of the test. At present an inadequate number of steels have been tested to allow an estimate of the general applicability of the test, and it is recommended that many more heats of steel be tested. It is desirable also to determine possible variations through a given heat of steel, for as is indicated in the data for steel Br, these variations may be quite great.

BIBLIOGRAPHY

1. Research Project SR-92, "Causes of Cleavage Failure in Ship Plate, Flat Plate Tests, and Additional Tests on Large Tubes" Serial No. SSC-8, Contract NObs-31222, dated January 17, 1947.

2. Research Project SR-93, "Cleavage Fracture of Ship Plates as Influenced by Size Effect", Serial No. SSC-10, Contract NObs-31224, dated June 12, 1947.

3. Research Project SR-96, "Correlation of Laboratory Tests with Full Scale Ship Plate Fracture Tests", Serial No. SSC-9, Contract NObs-31217, dated March 17, 1947.

4. Research Project SR-96, "Correlation of Laboratory Tests with Full Scale Ship Plate Fracture Tests", Serial No. SSC-15, Contract NObs-31217, dated December 31, 1947.

5. "The Notched Bar Impact Test According to Schnadt" (Abstracted from De Ingenieur, Volume 50, Number 50, December 13, 1946). Engineer's Digest, March 1947.

TABLE I

Comparison of Estimated Transition Temperatures of Slow-Bend Notched-Bar Tests and 72" Wide Notched Tension Tests

			TRANSITION TEMPERATURE - °F Steel									
TYPE OF TEST	SPECIMEN ORIENTATION	DATA USED	E	C	A	Dr	Dn	Bn	Br	Q	H	N
72" wide tension	-	50% Energy absorption Ref. 1 & 2	100	90	35	30	28	31	32		20	-45
Slow-bend notched-bar tost	LH, except as noted	Energy absorption Ref. 4	73	97	50	19	23	30	BH -4	-11	BH 18	-35
Slow-bend notched-bar Schnadt Type	LH	$w_o - w_1$	85	110	50	25	25	25	-25	-20	-35	-30
Slow-bend notched-bar Schnadt Type	LH	% Ductile Fracture	85	120	50	25	25	25	-25	-15	-35	-30
Slow-bend notched-bar Schnadt Type	BH	$w_o - w_1$	70	100+	40	25	20	-	-20	-15	-10	-15
Slow-bend notched-Bar Schnadt Type	BH	% Ductile Fracture	70	100+	40	25	20	-	-20	-15	-10	-15

TABLE II

Steel	Large Plate #	Transition Temperature .788 x 3/4" V-notch, 1/2" Drilled Hole*
A	A1A	60°F
A	A2A	25°F
A	A3A	45°F
Bn	B4A	+32°F
Br	B1A	+30°F
C	C1A	95°F
C	C2A	120°F
Dr	18A1K	25°F
Dn	5-7	10°F
E	13A7	110°F

* All specimens were of LH orientation and transition temperatures were picked on the basis of $w_0 - w_1$ values. Specimens were selected from relatively unstrained material immediately under the notch of the 72" wide flat plate specimen.

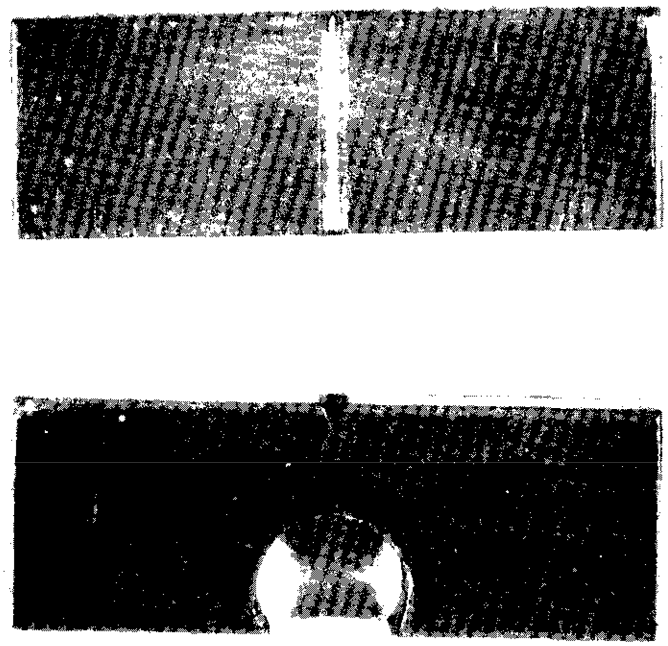

Figure 1 Photograph of "Schnadt Type" Slow **Bend**
Notched Bar Test.

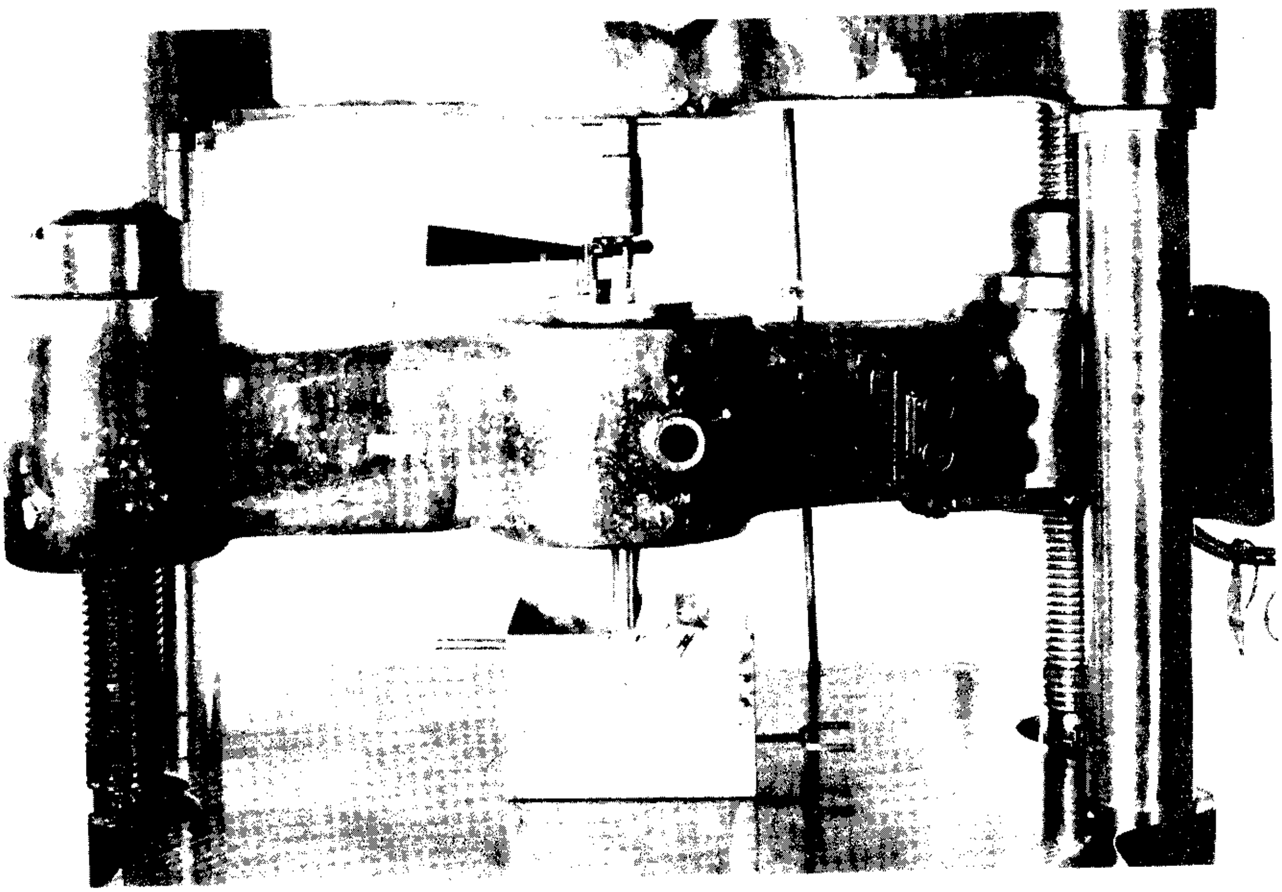

Figure 2 Photograph of Equipment
General Assembly

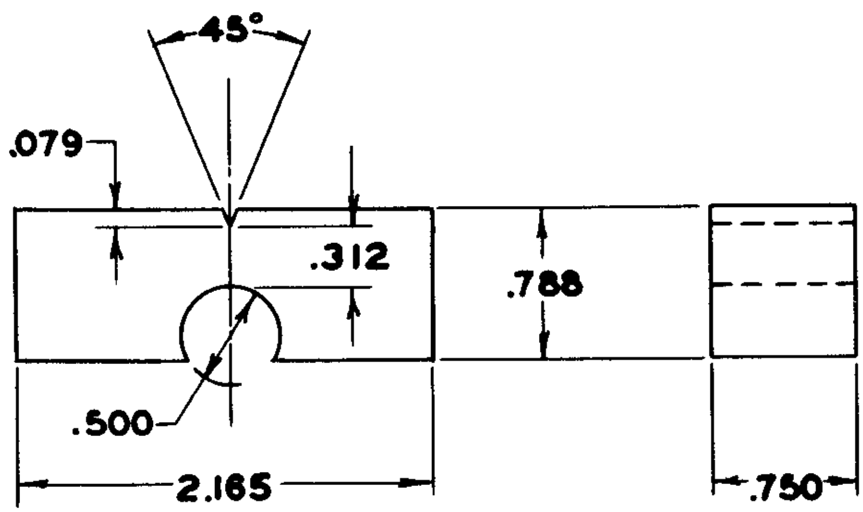

SLOW BEND TEST

COMPRESSION ZONE REMOVED

FIG. 3

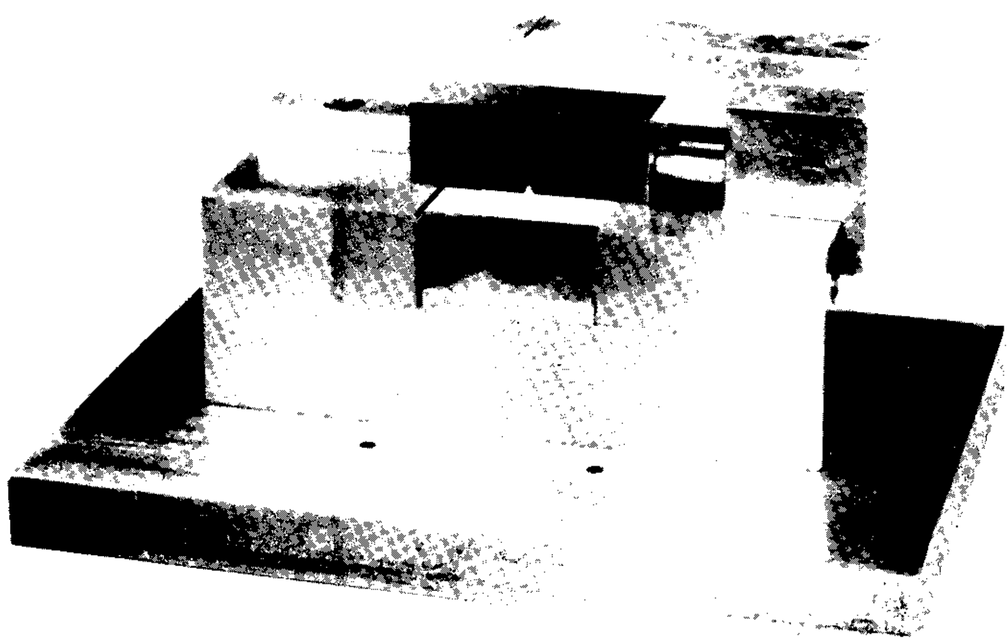

Figure 4

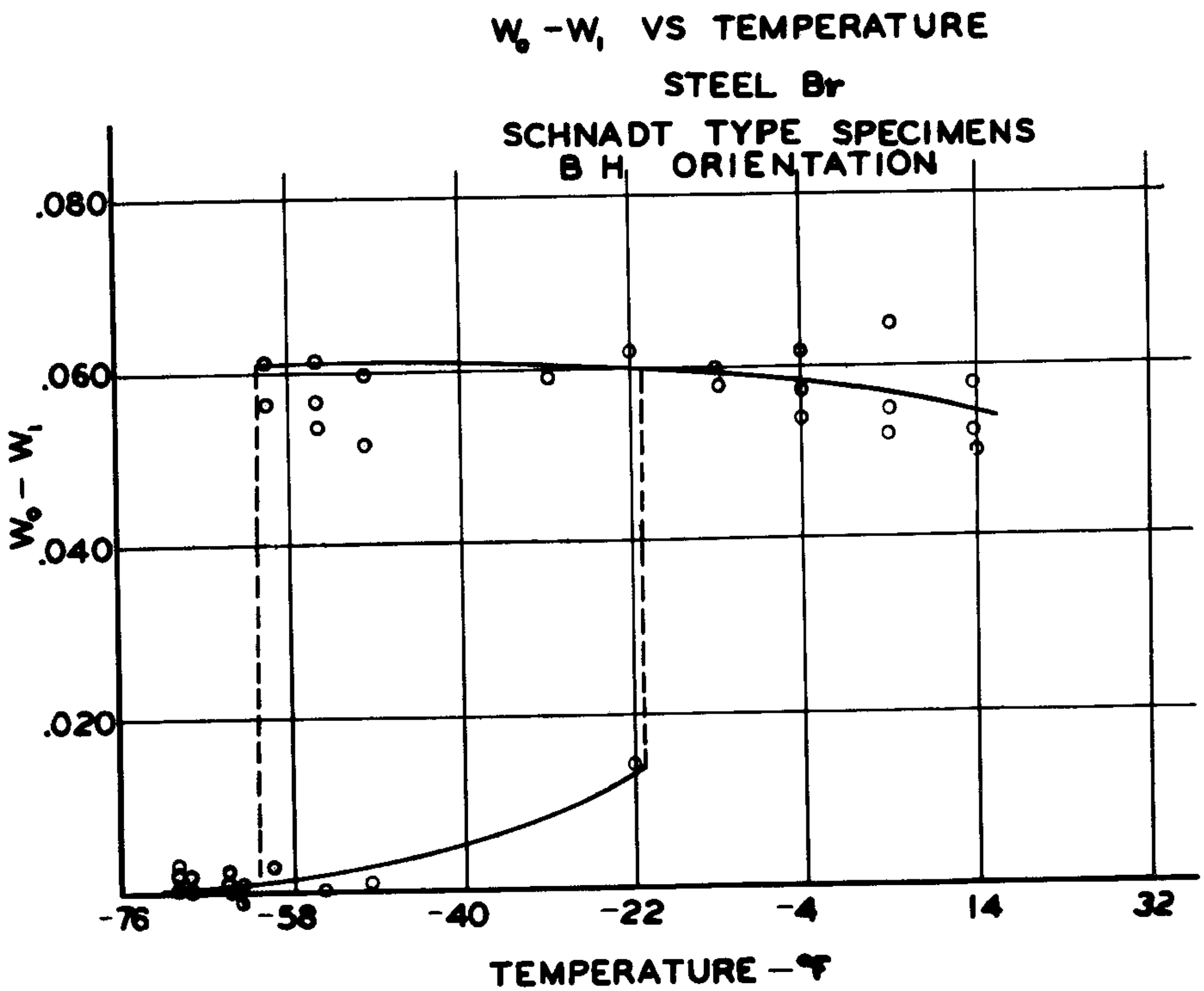
W₀ - W₁ VS TEMPERATURE
STEEL Br
SCHNADT TYPE SPECIMENS
B H ORIENTATION
.080
.060
.040
.020
W₀ - W₁
-76
-58
-40
-22
-4
14
32
TEMPERATURE — °F

FIGURE 5

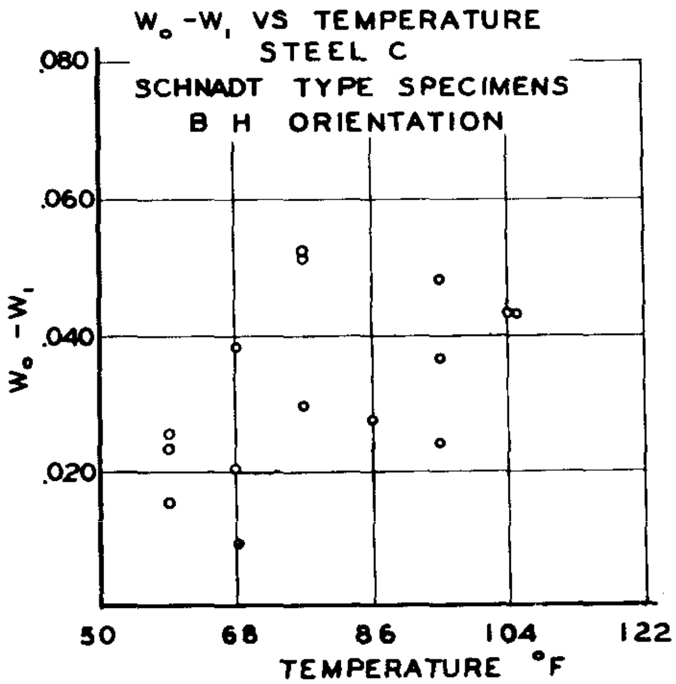

FIGURE 6

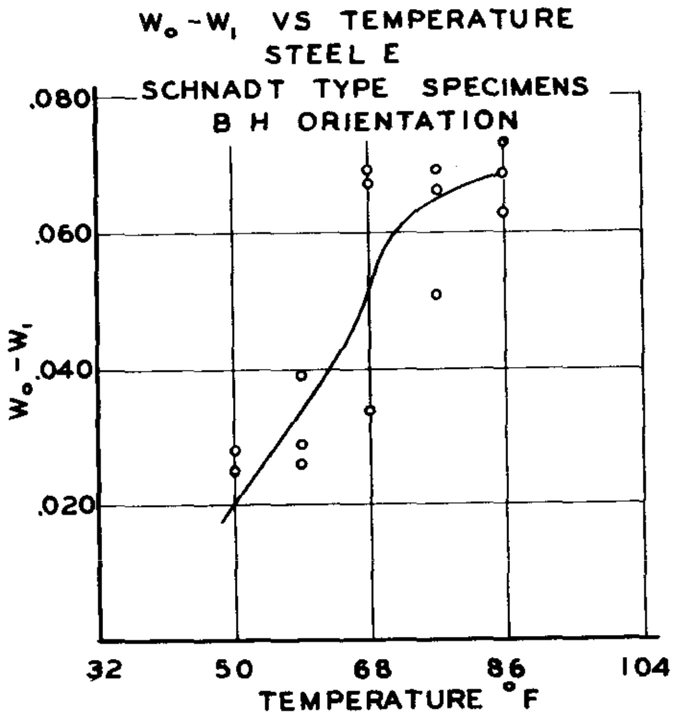

FIGURE 7

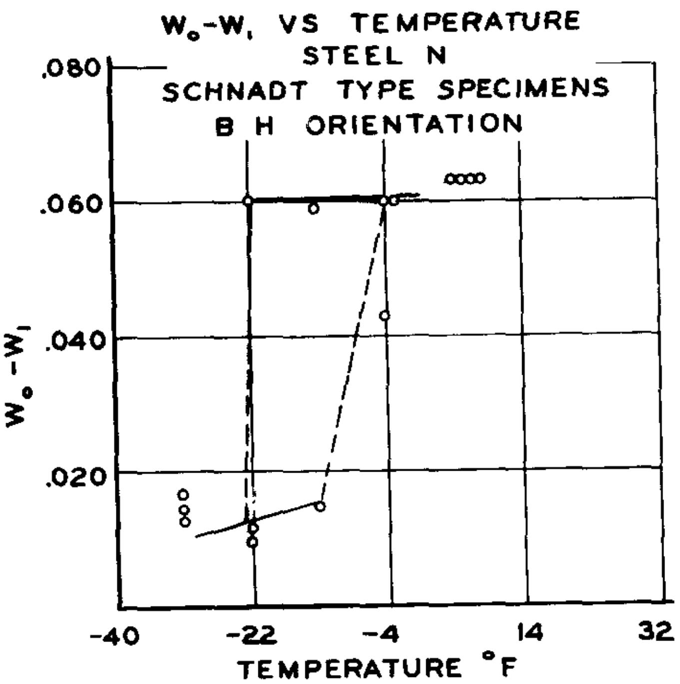

FIGURE 8

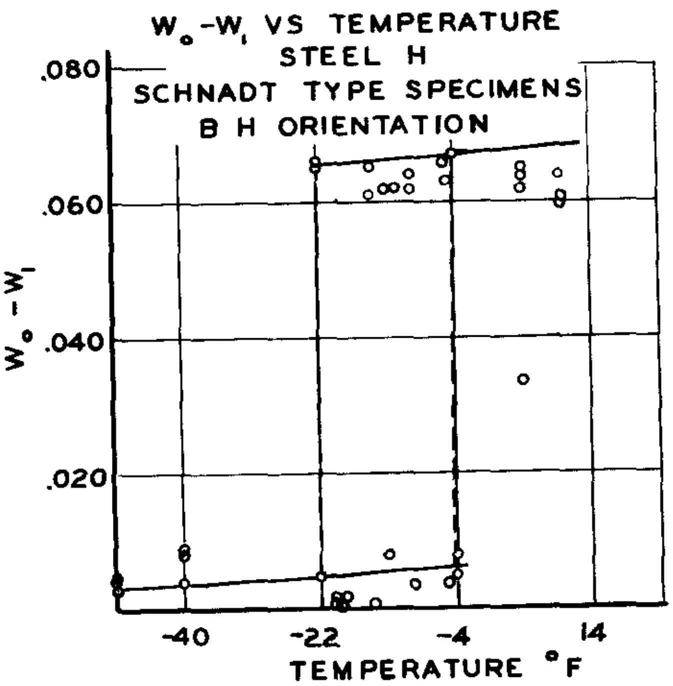

FIGURE 9

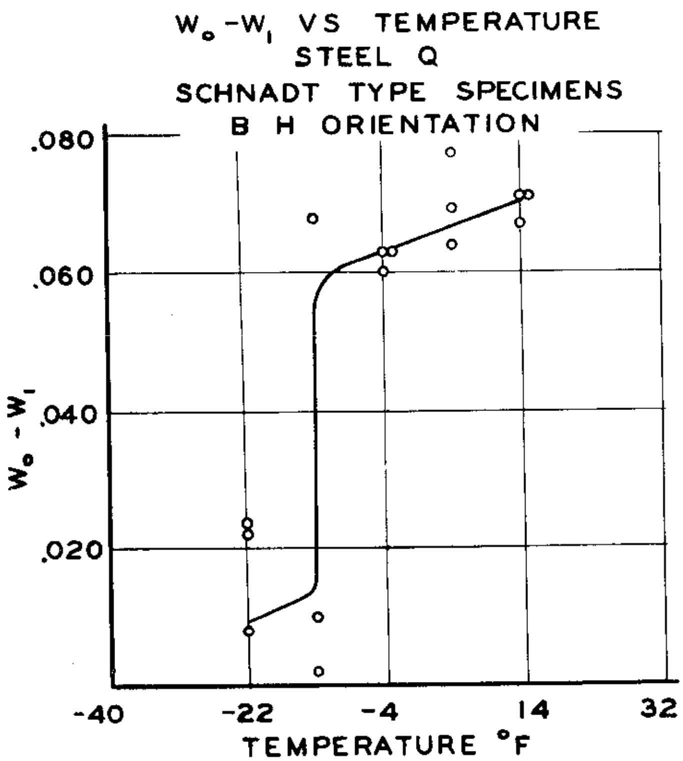

FIGURE 10

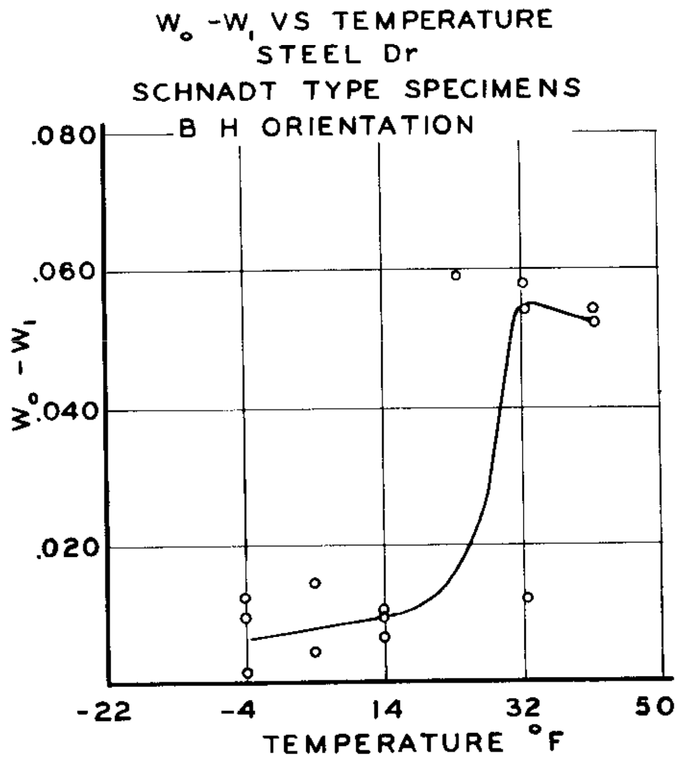

FIGURE 11

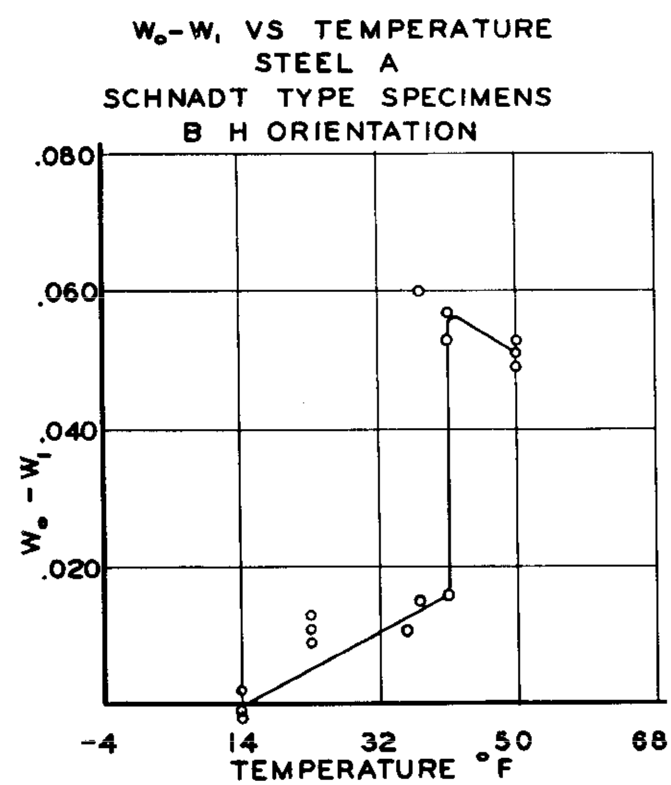

FIGURE 12

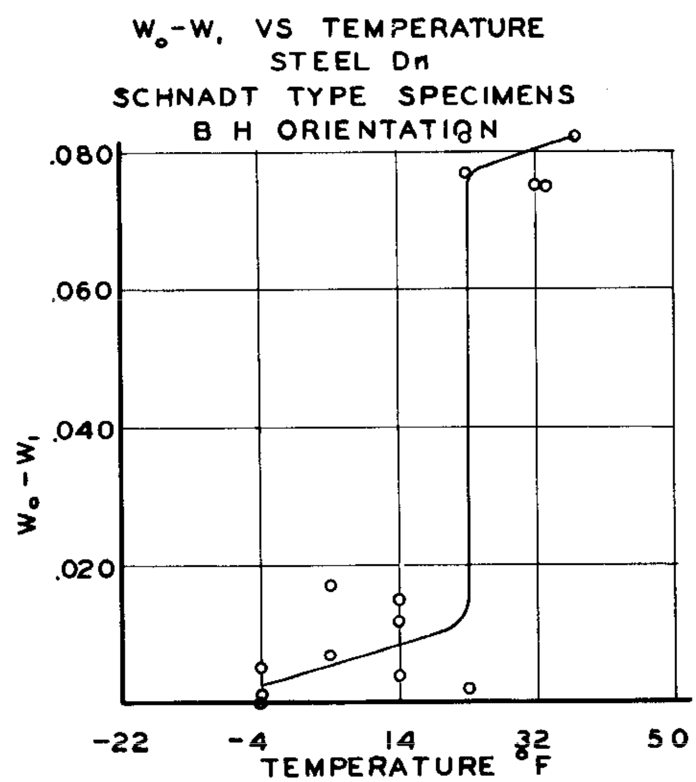

FIGURE 13

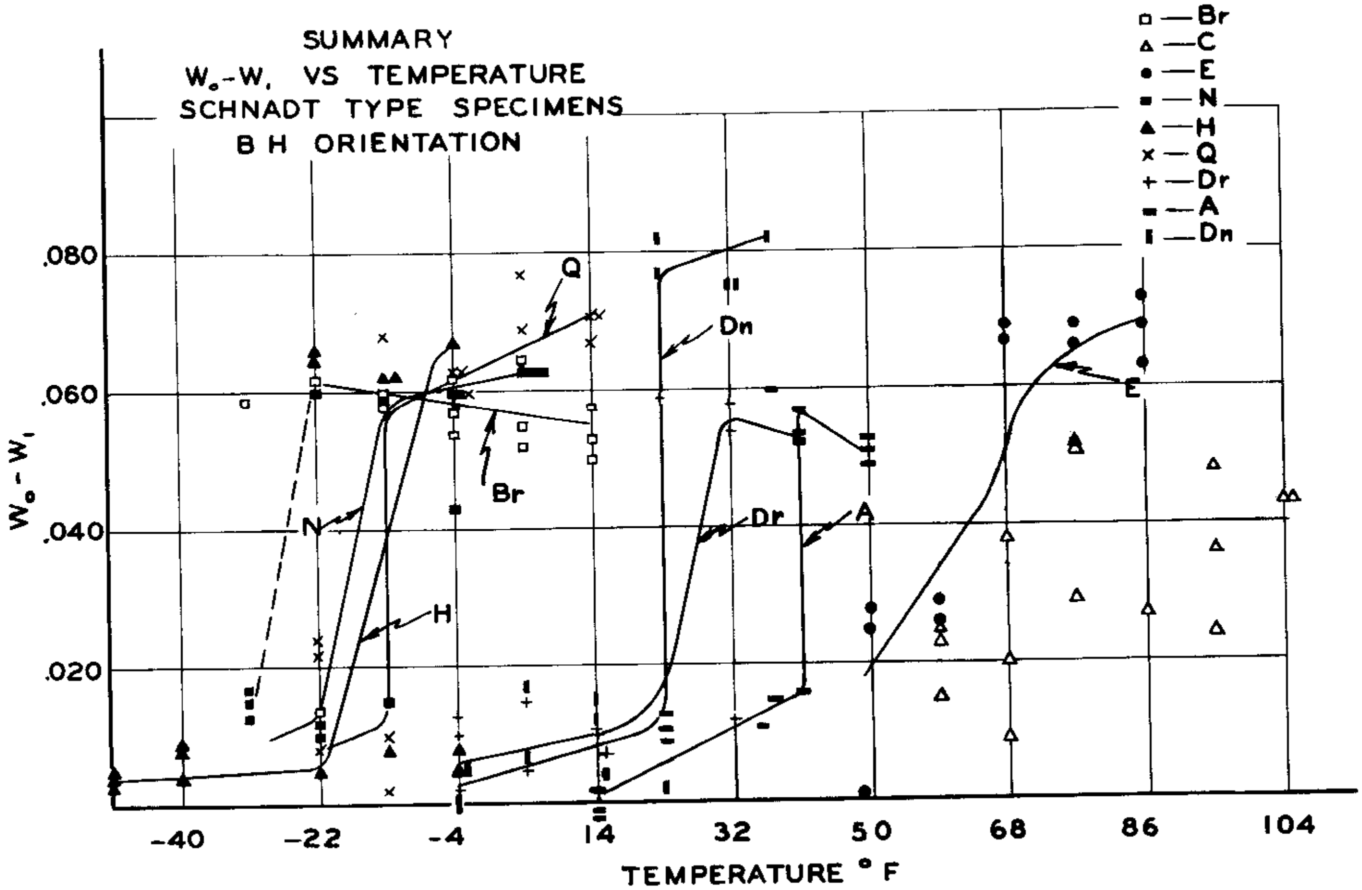

FIGURE 14

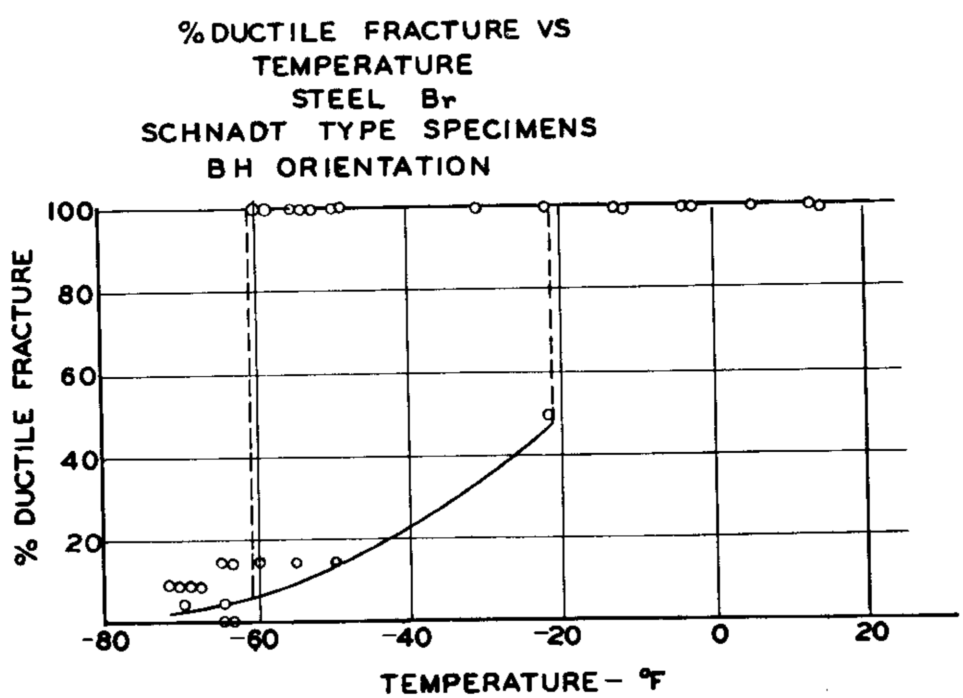

FIGURE 15

% DUCTILE FRACTURE VS TEMPERATURE
STEEL E
SCHNADT TYPE SPECIMENS
BH ORIENTATION

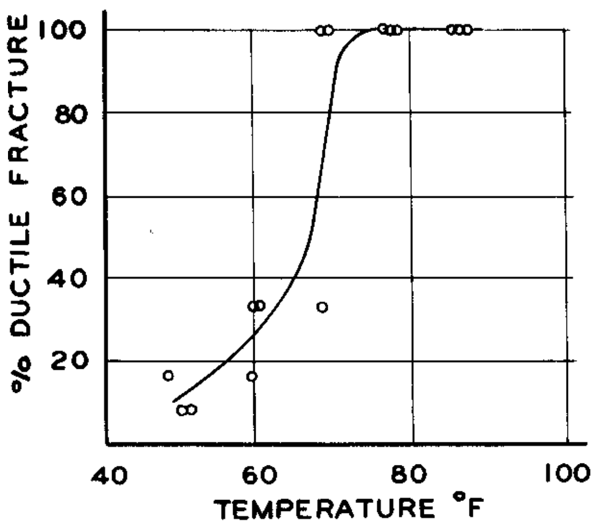

FIGURE 16

% DUCTILE FRACTURE VS TEMPERATURE
STEEL C
SCHNADT TYPE SPECIMENS
BH ORIENTATION

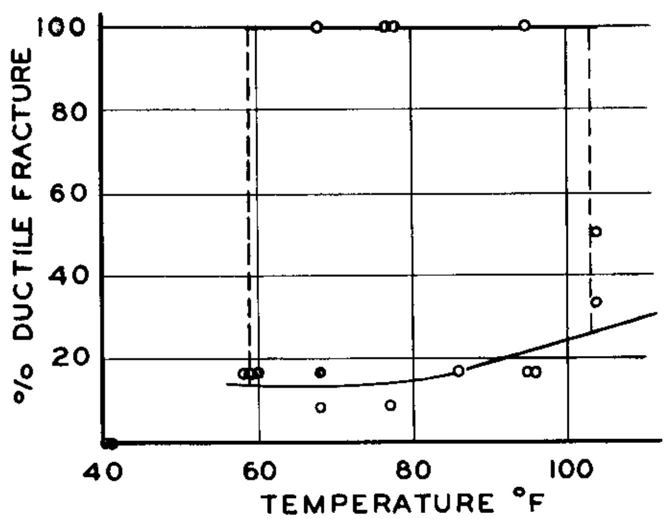

FIGURE 17

% DUCTILE FRACTURE VS TEMPERATURE
STEEL N
SCHNADT TYPE SPECIMENS
BH ORIENTATION

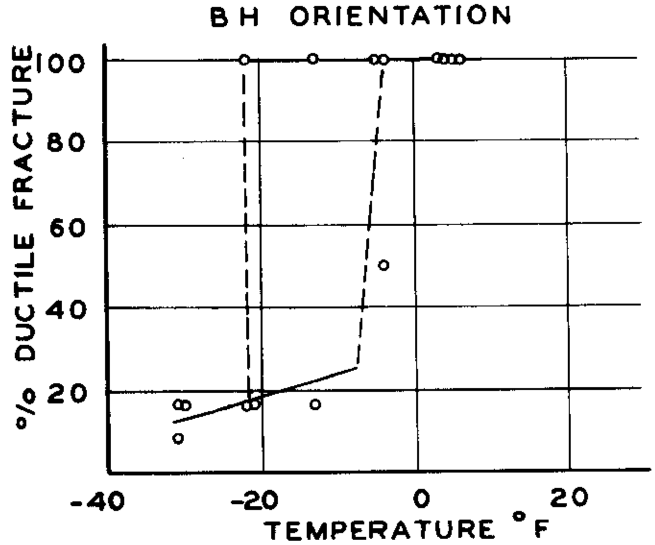

FIGURE 18

% DUCTILE FRACTURE VS TEMPERATURE
STEEL H
SCHNADT TYPE SPECIMENS
BH ORIENTATION

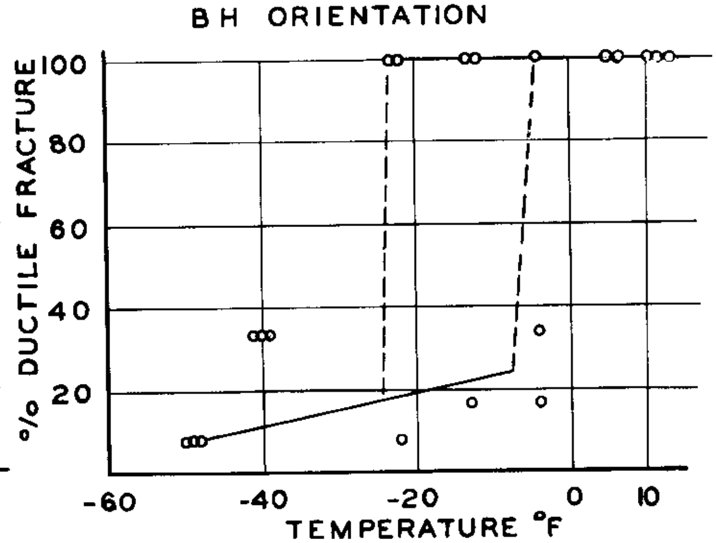

FIGURE 19

% DUCTILE FRACTURE VS
TEMPERATURE
STEEL Dr
SCHNADT TYPE SPECIMENS
BH ORIENTATION

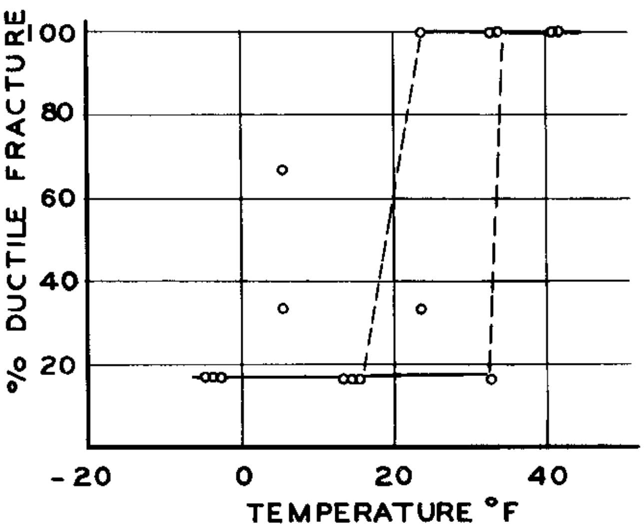

FIGURE 20

% DUCTILE FRACTURE VS
TEMPERATURE
STEEL Q
SCHNADT TYPE SPECIMENS
BH ORIENTATION

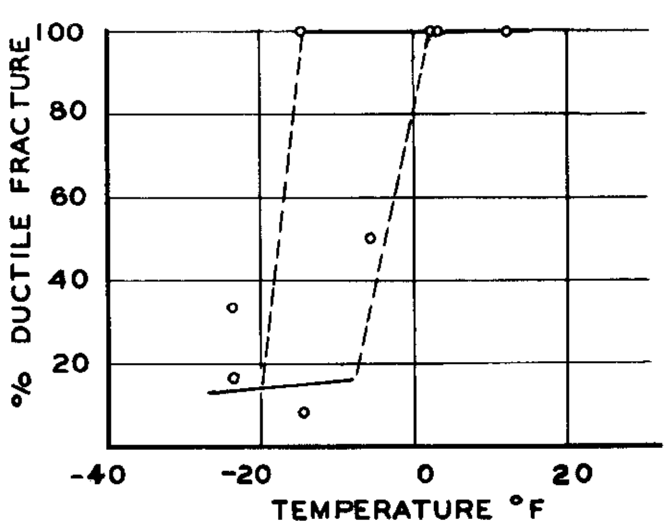

FIGURE 21

% DUCTILE FRACTURE VS
TEMPERATURE
STEEL A
SCHNADT TYPE SPECIMENS
BH ORIENTATION

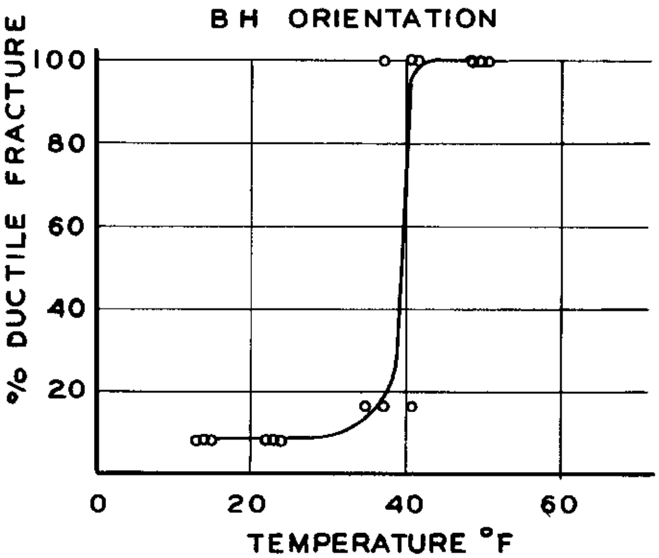

FIGURE 22

% DUCTILE FRACTURE VS
TEMPERATURE
STEEL Dn
SCHNADT TYPE SPECIMENS
BH ORIENTATION

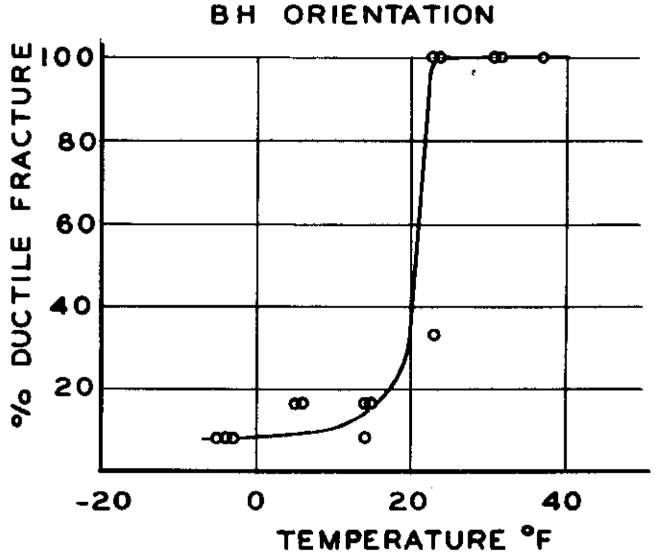

FIGURE 23

SUMMARY
% DUCTILE FRACTURE VS TEMPERATURE
SCHNADT TYPE SPECIMENS
B H ORIENTATION

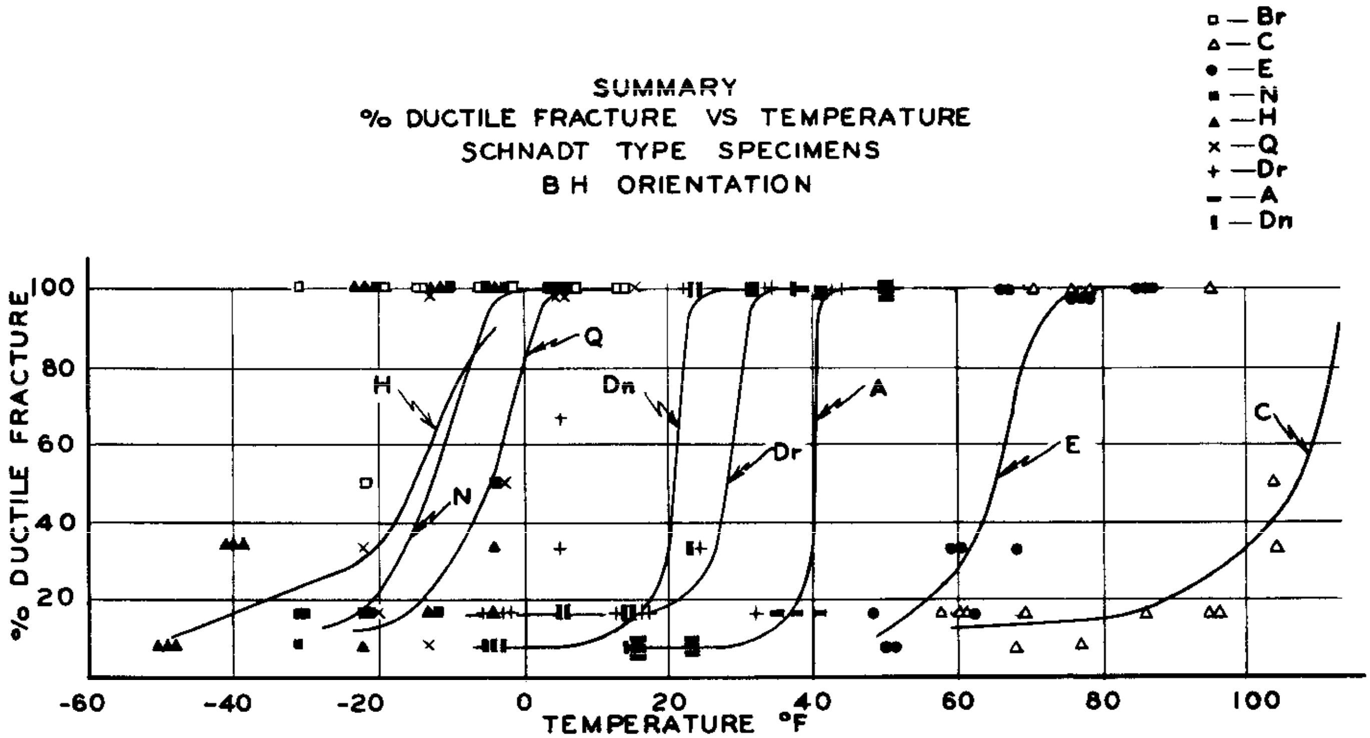

FIGURE 24

$W_o - W_i$ VS TEMPERATURE
STEEL Br
SCHNADT TYPE SPECIMENS
L H ORIENTATION

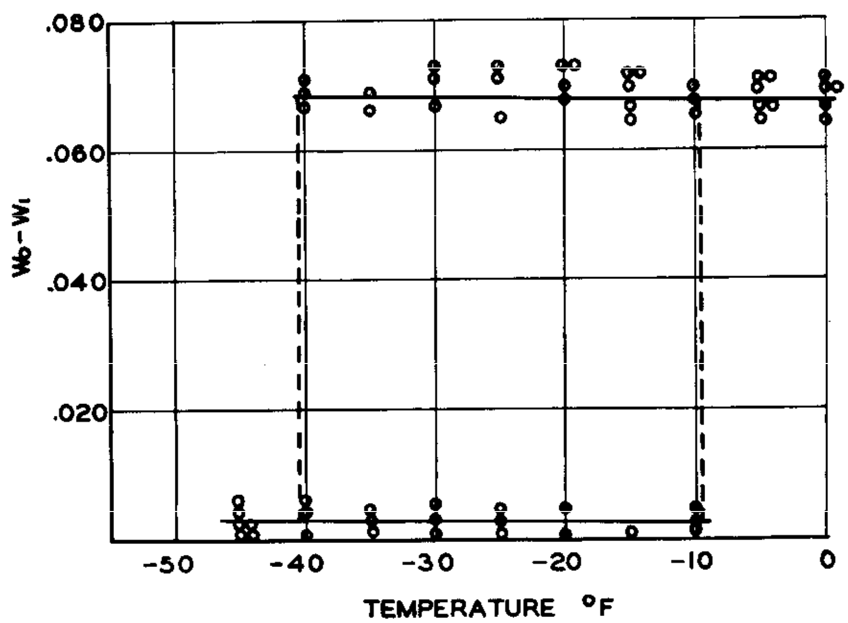

FIGURE 25

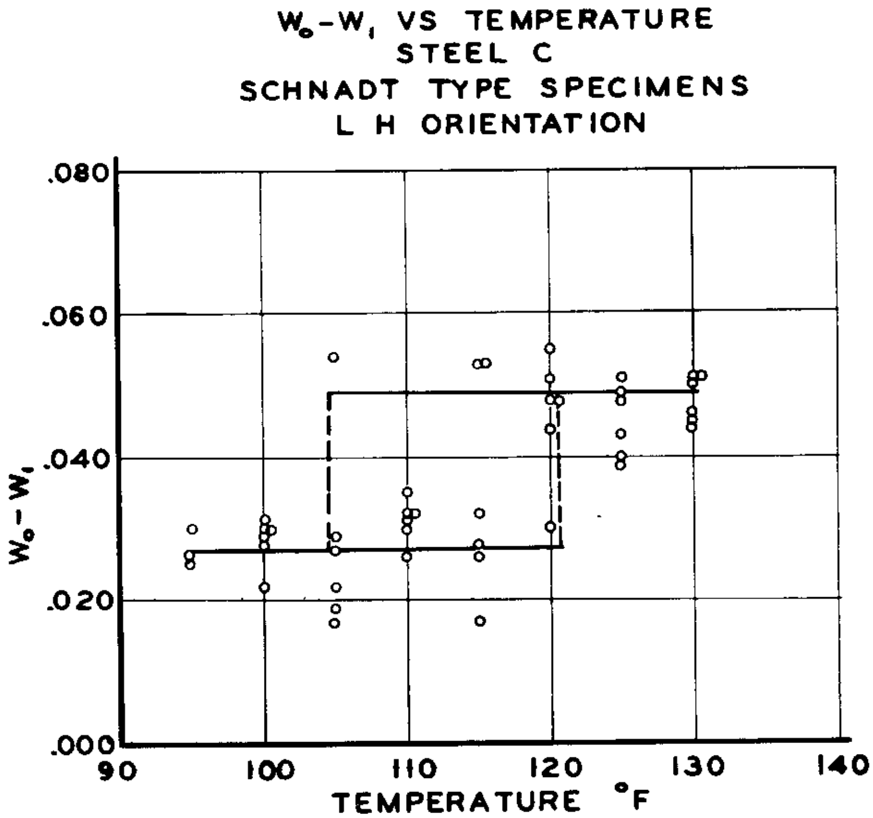

FIGURE 26

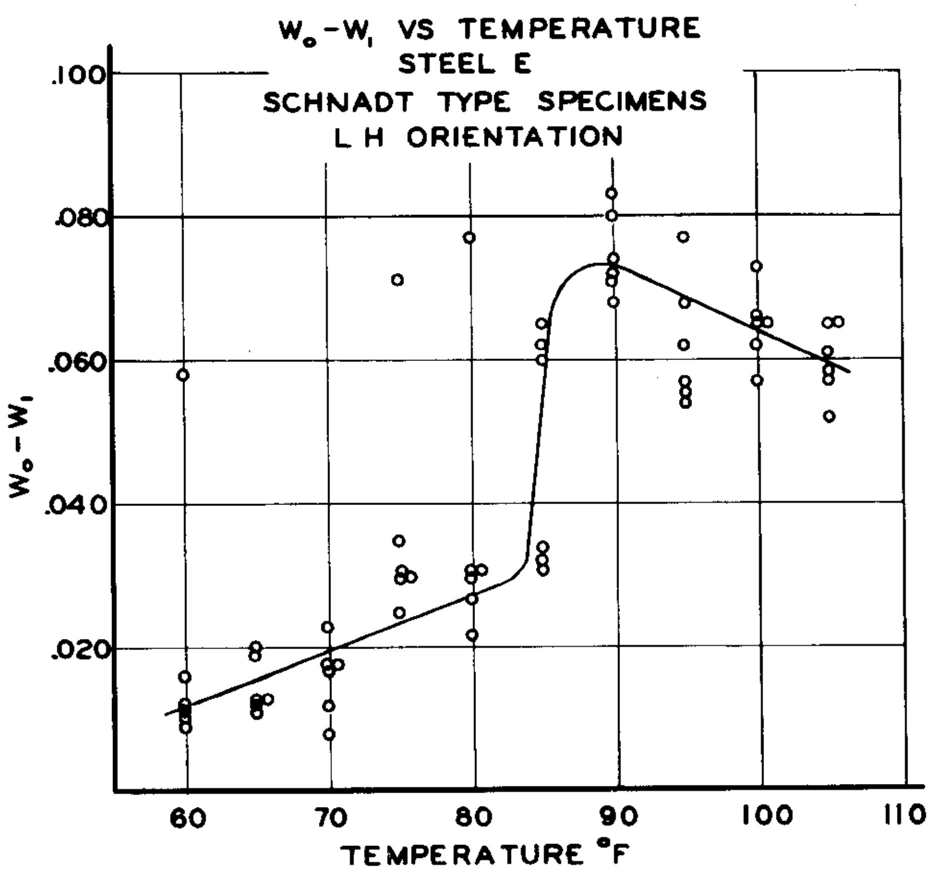

FIGURE 27

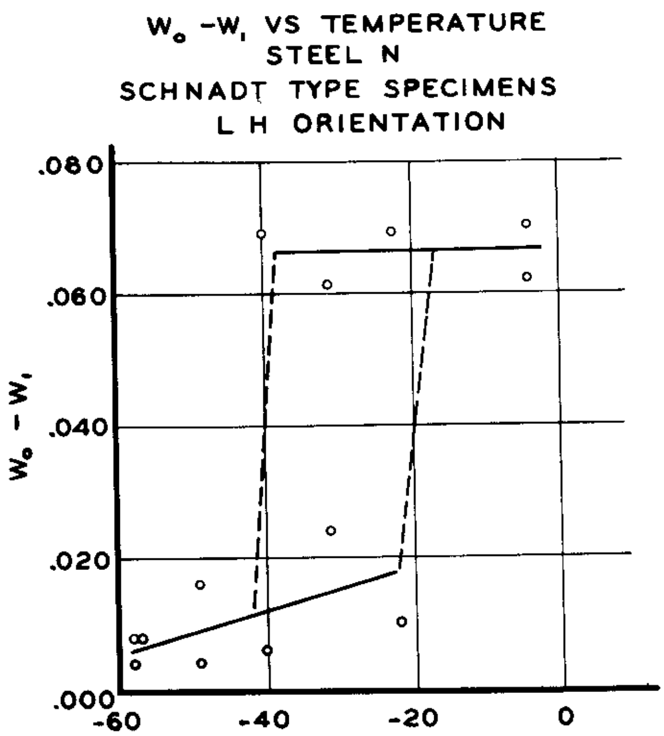

FIGURE 28

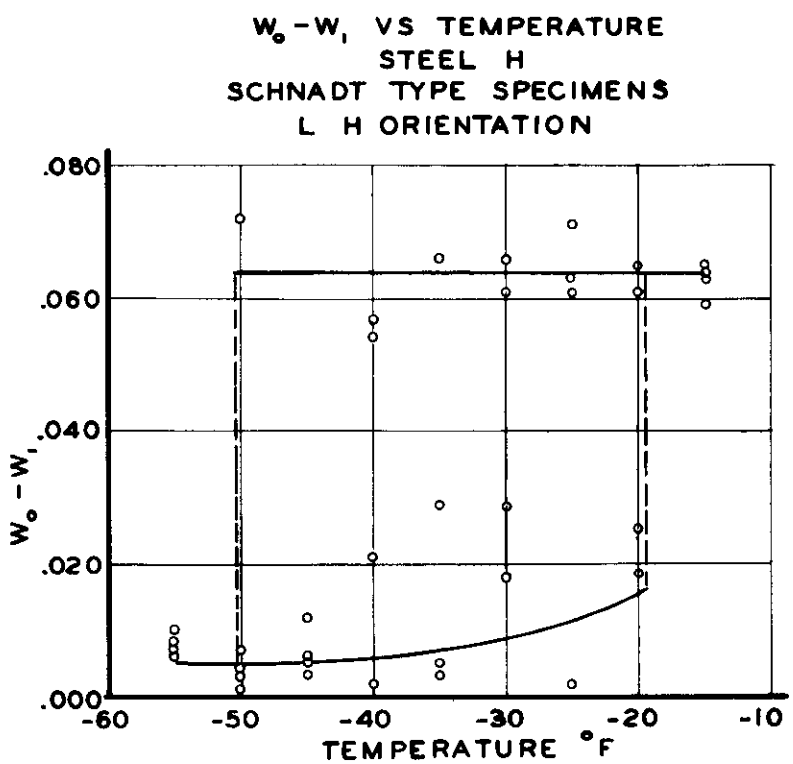

FIGURE 29

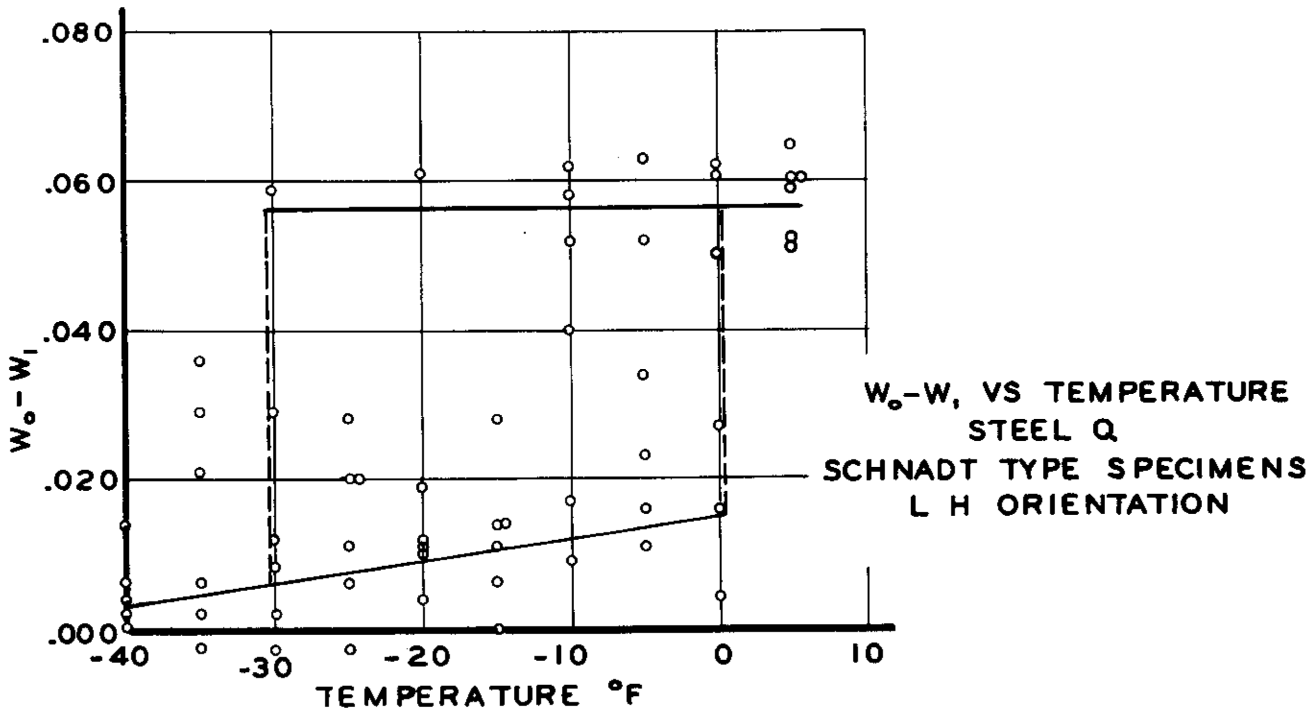

FIGURE 30

W_o-W_1 VS TEMPERATURE
STEEL Dr
SCHNADT TYPE SPECIMENS
L H ORIENTATION

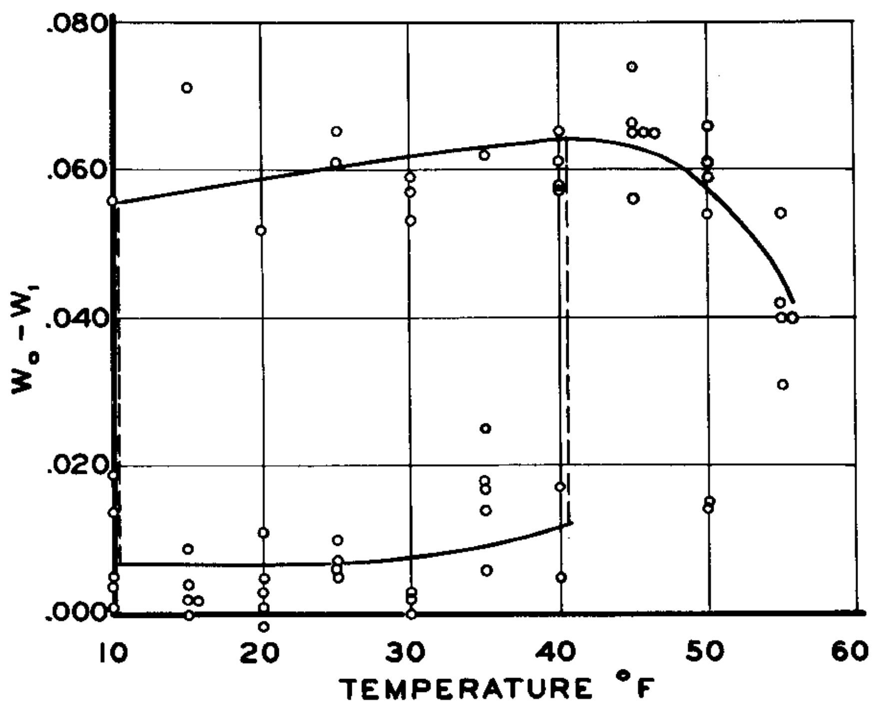

FIGURE 31

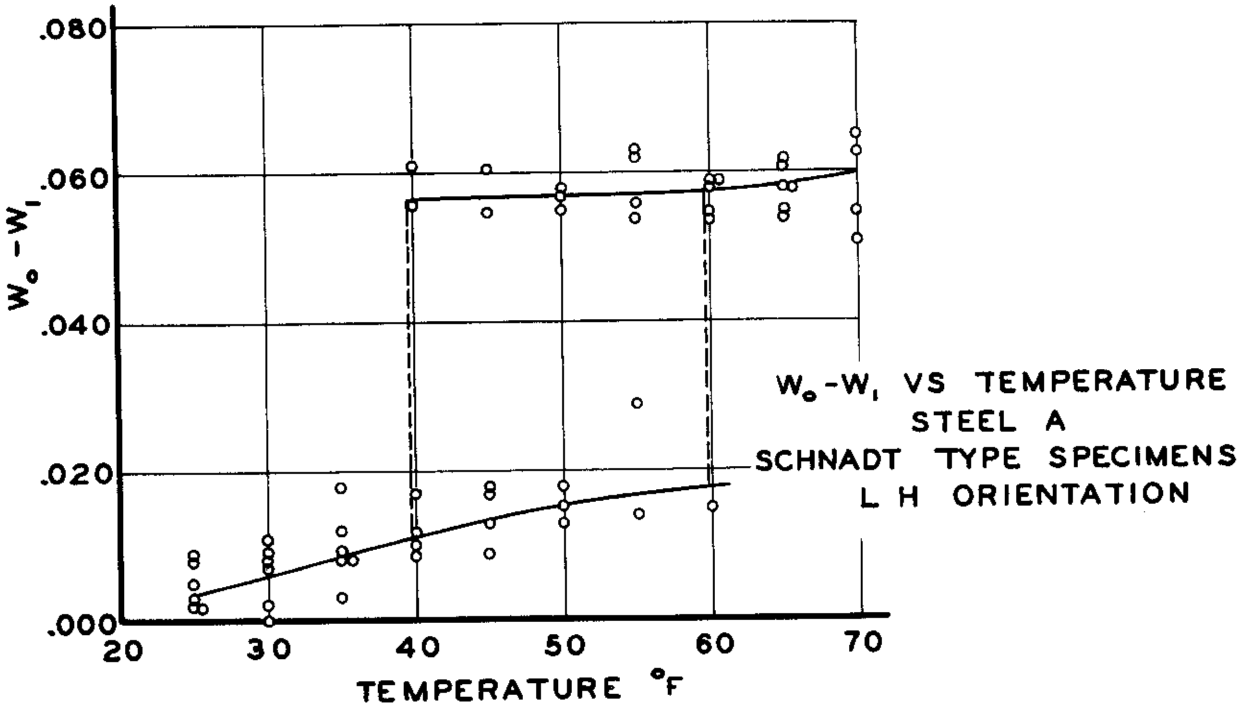

FIGURE 32

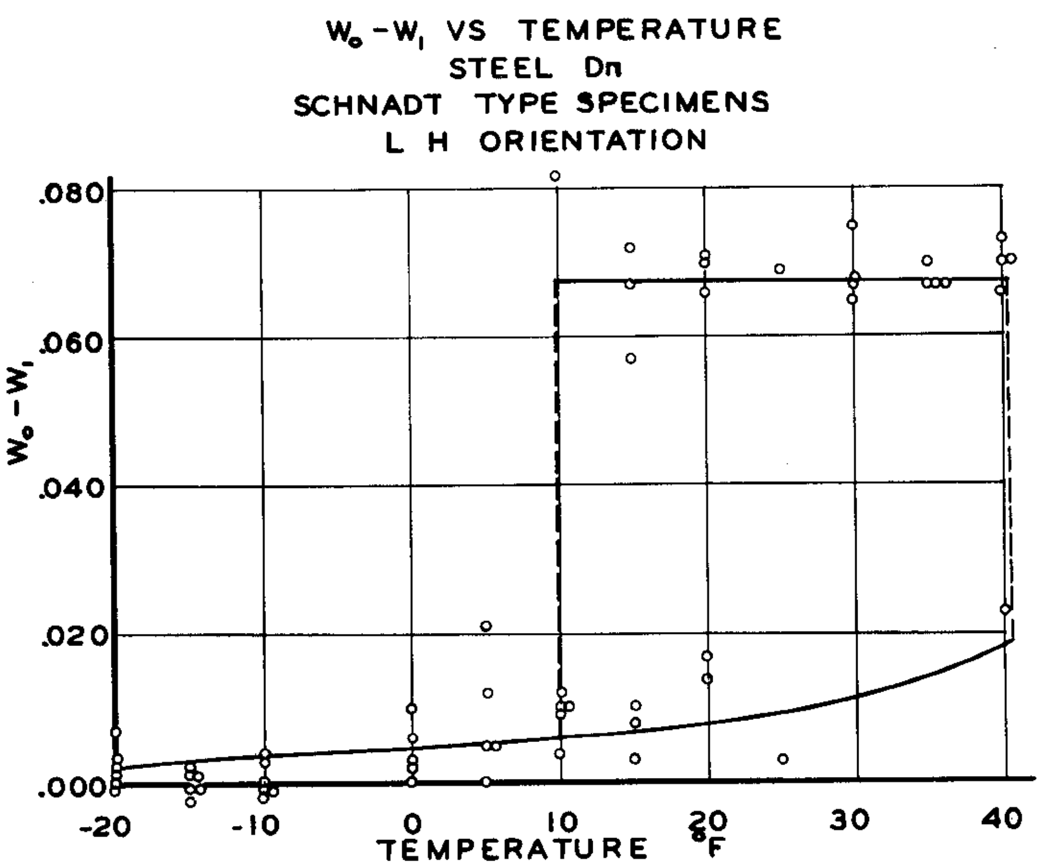

FIGURE 33

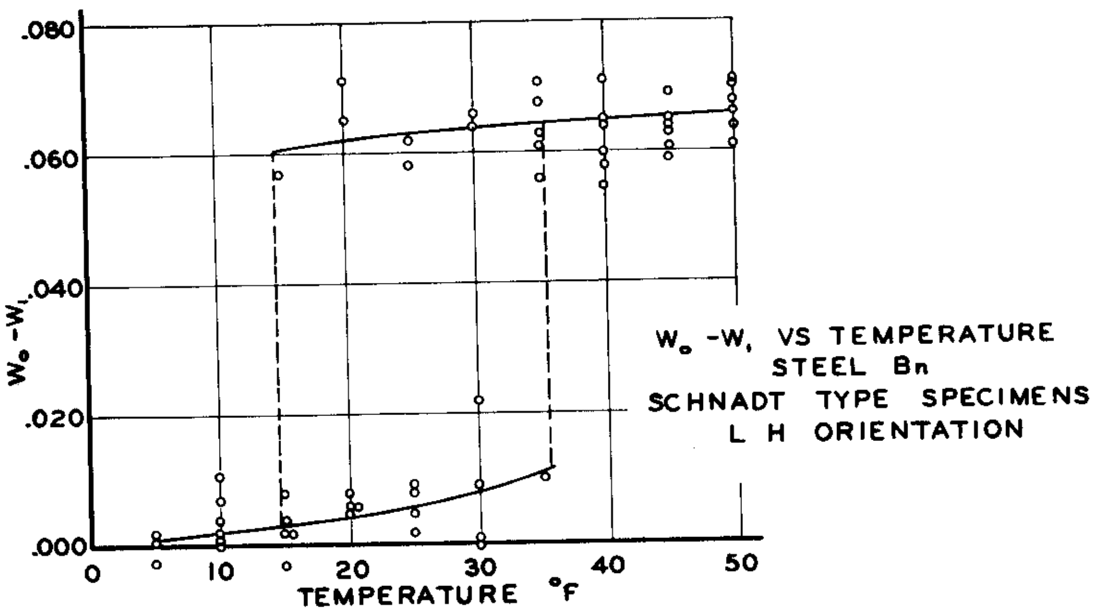

FIGURE 34

SUMMARY
$W_o - W_1$ VS TEMPERATURE
SCHNADT TYPE SPECIMENS
L H ORIENTATION

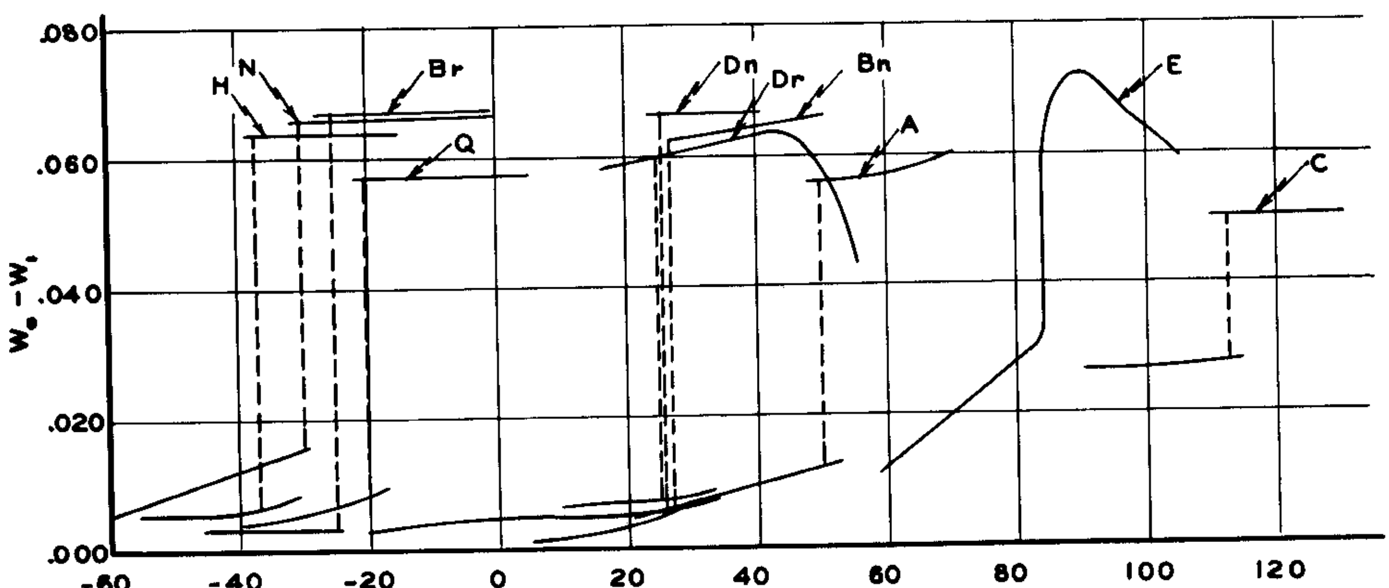

FIGURE 35

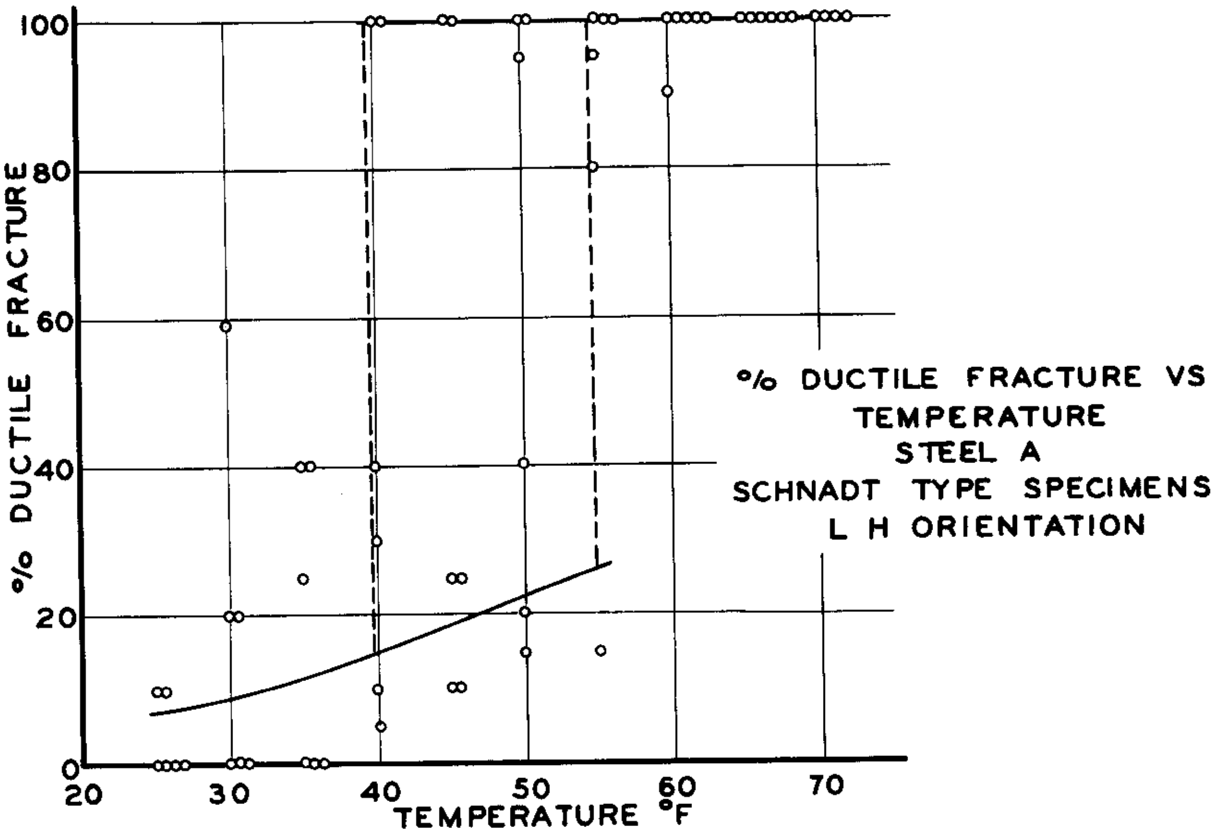

FIGURE 36

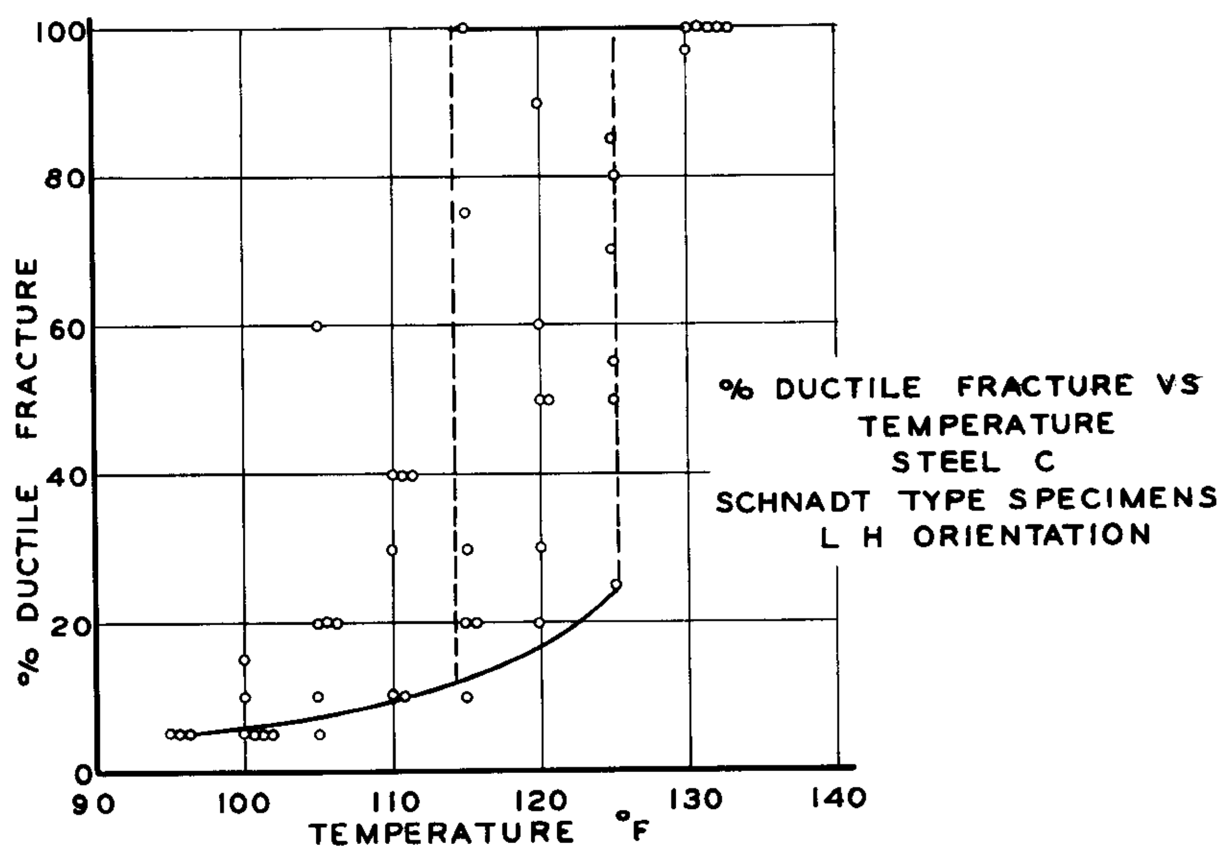

FIGURE 37

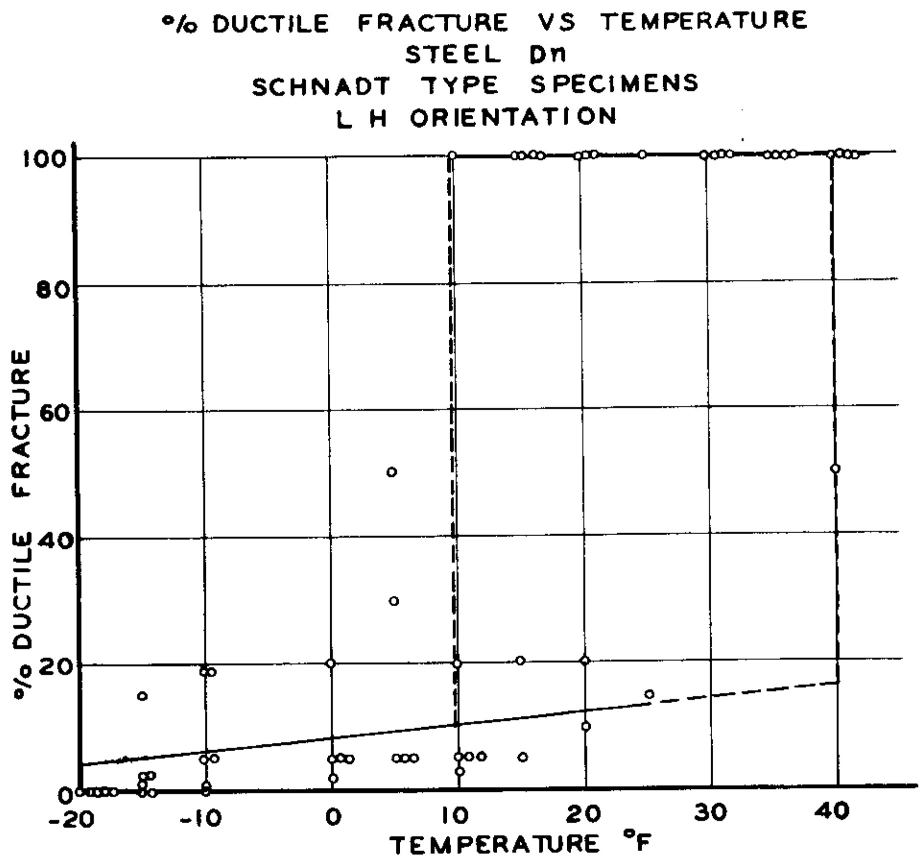

FIGURE 38

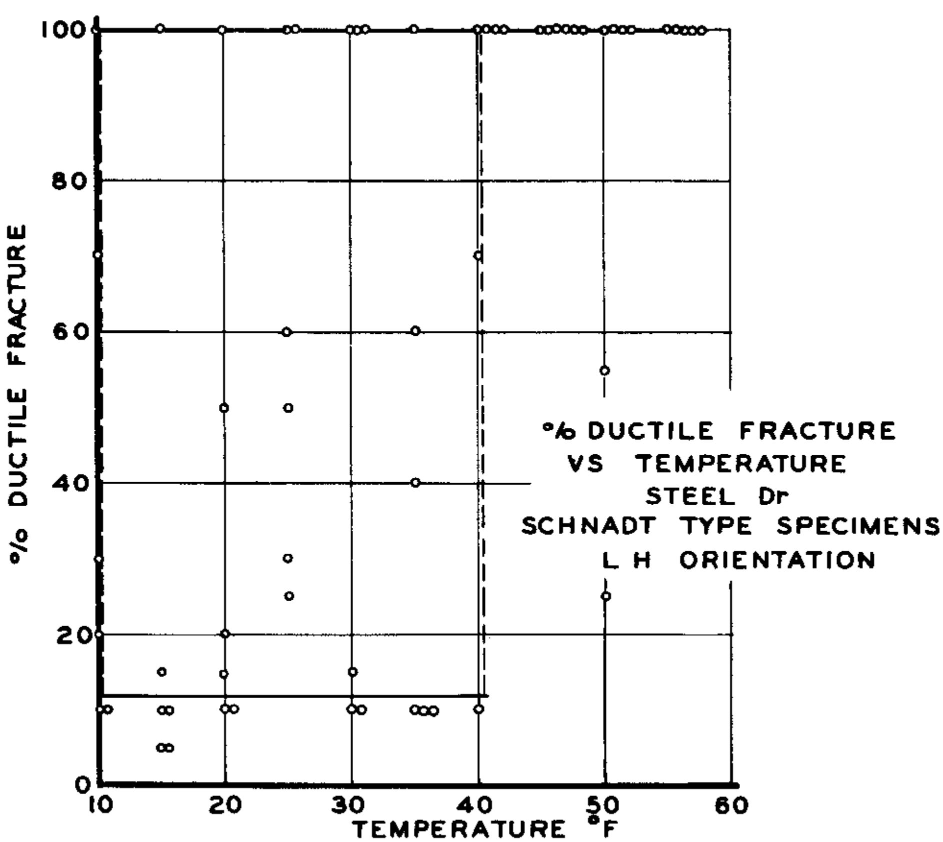

FIGURE 39

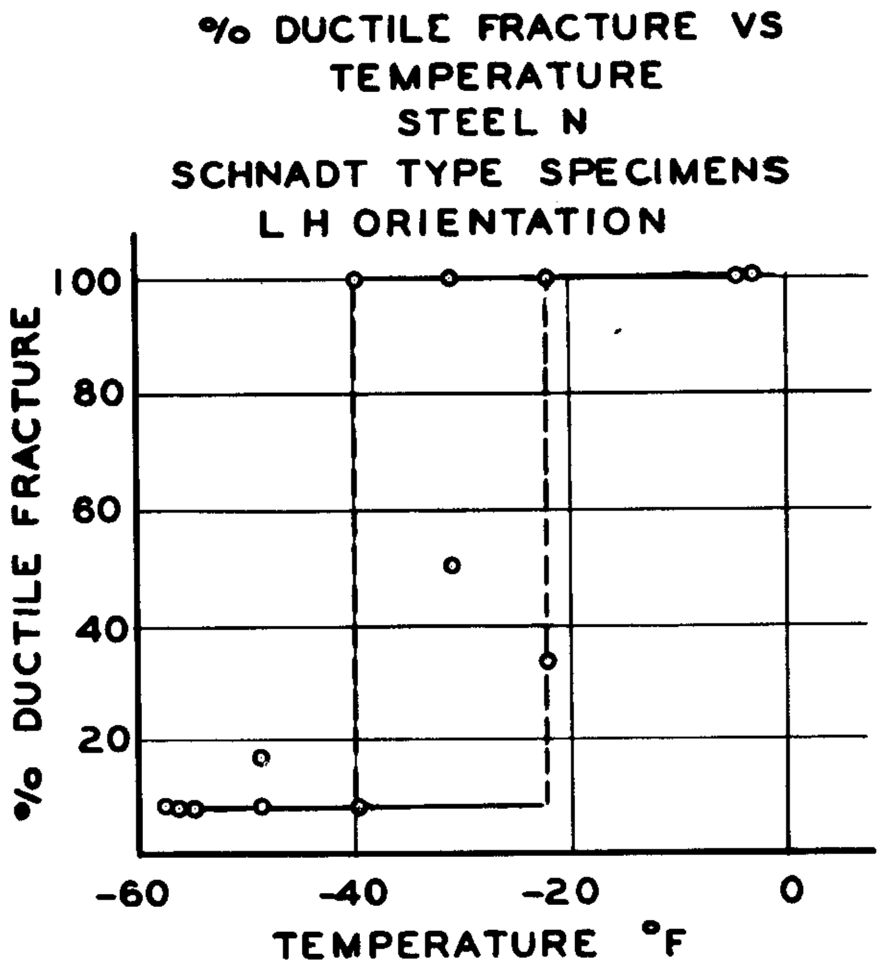
% DUCTILE FRACTURE VS
TEMPERATURE
STEEL N
SCHNADT TYPE SPECIMENS
L H ORIENTATION
% DUCTILE FRACTURE
100
80
60
40
20
-60
-40
-20
0
TEMPERATURE °F

FIGURE 40

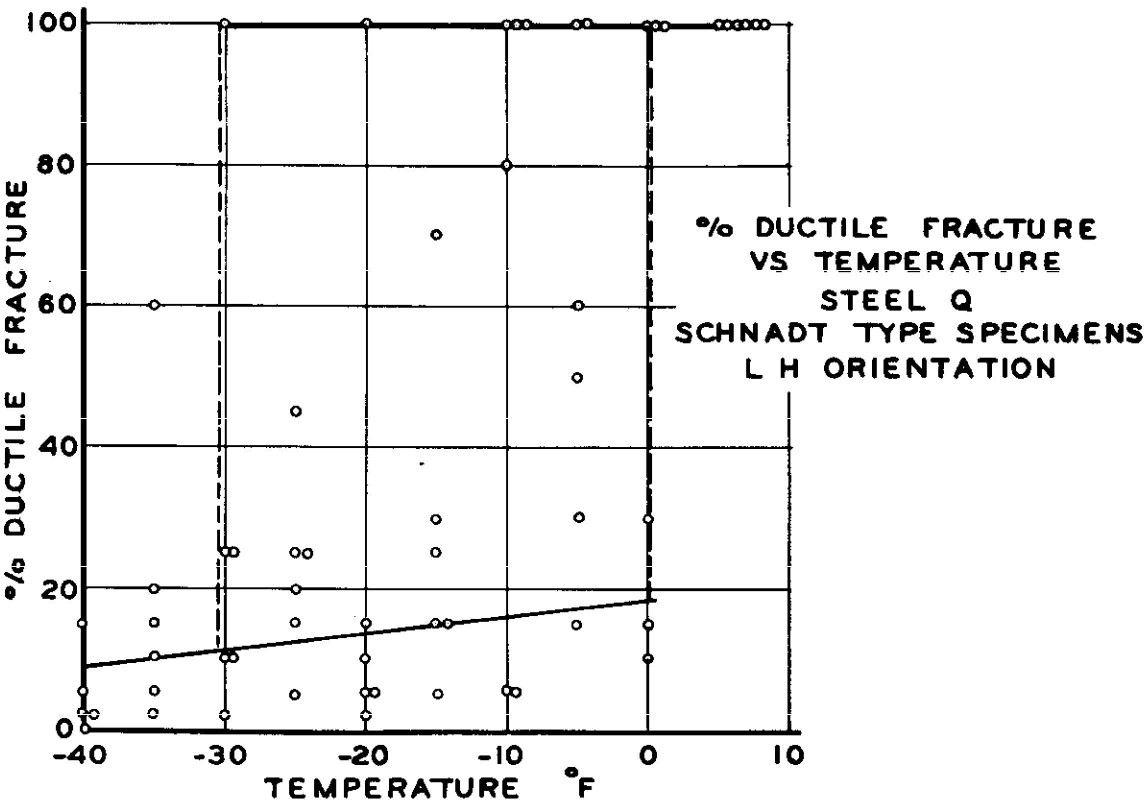

FIGURE 41

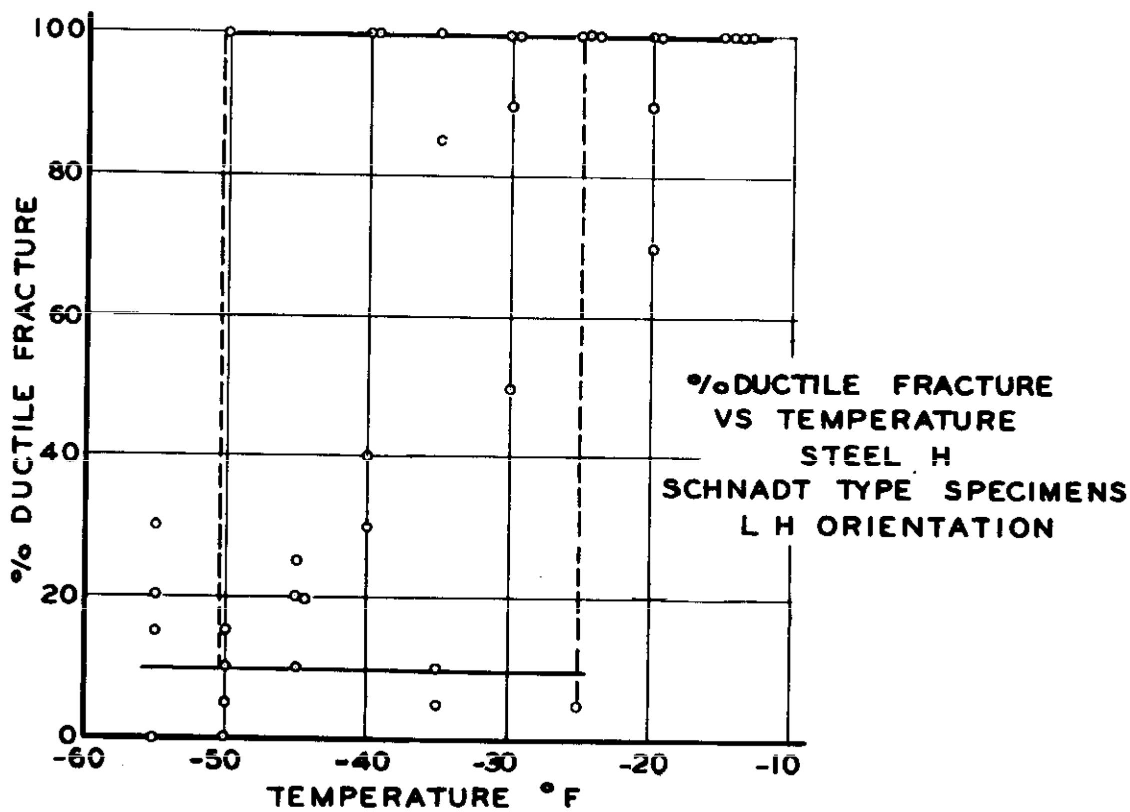

FIGURE 42

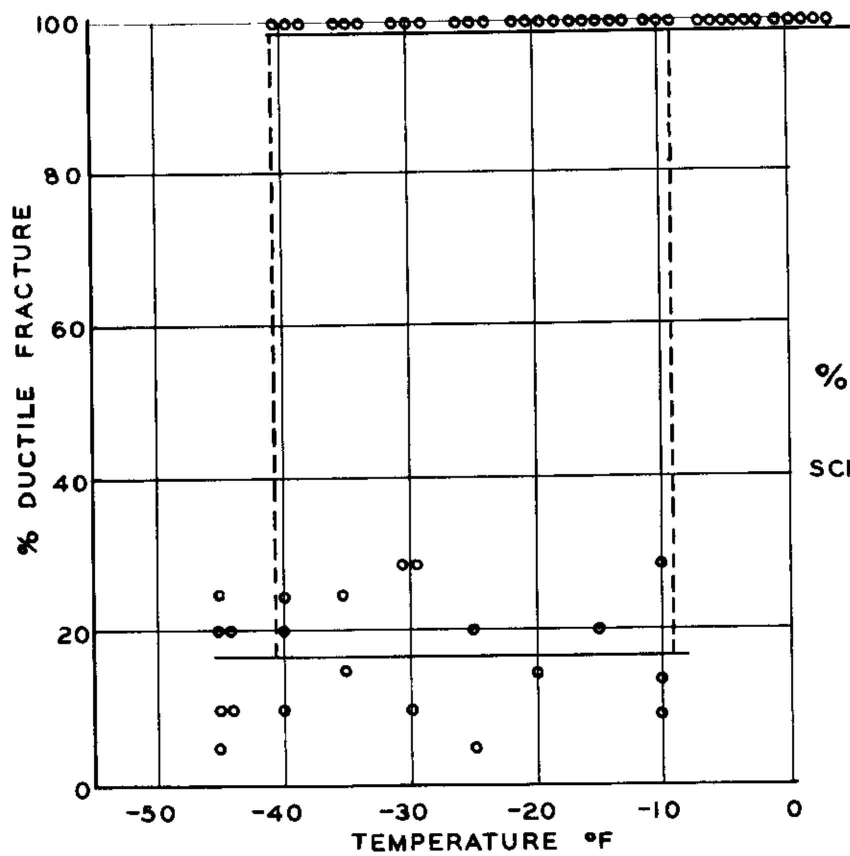

% DUCTILE FRACTURE VS
TEMPERATURE
STEEL Br
SCHNADT TYPE SPECIMENS
L H ORIENTATION

FIGURE 43

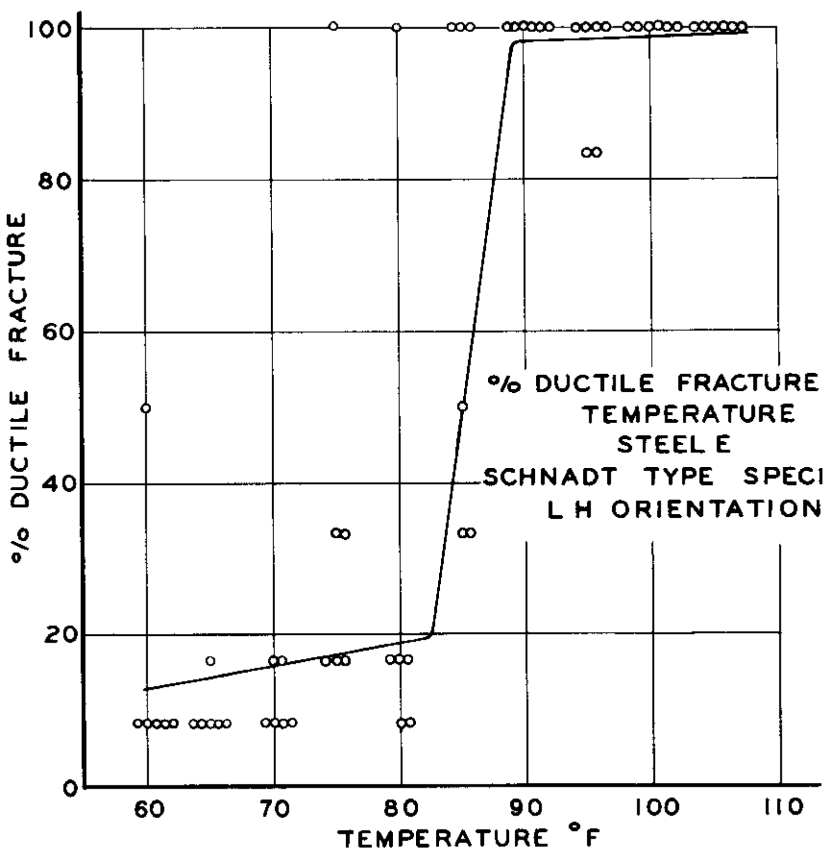

% DUCTILE FRACTURE VS
TEMPERATURE
STEEL E
SCHNADT TYPE SPECIMENS
L H ORIENTATION

FIGURE 44

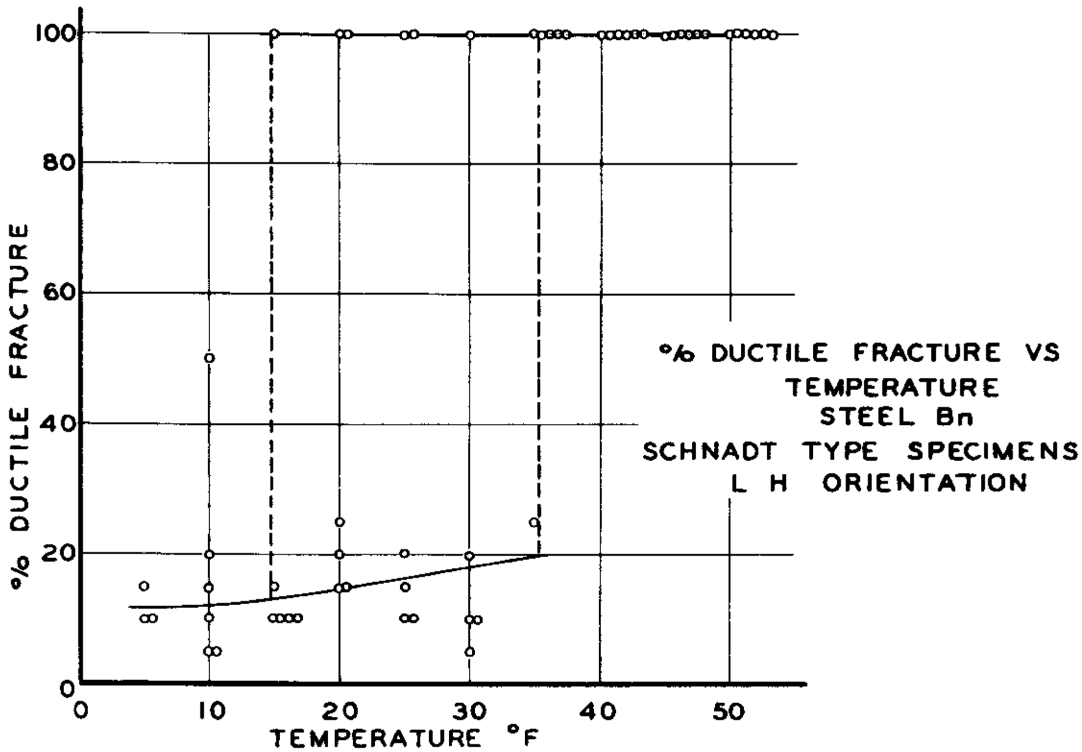

FIGURE 45

SUMMARY
% DUCTILE FRACTURE VS TEMPERATURE
SCHNADT TYPE SPECIMENS
L H ORIENTATION

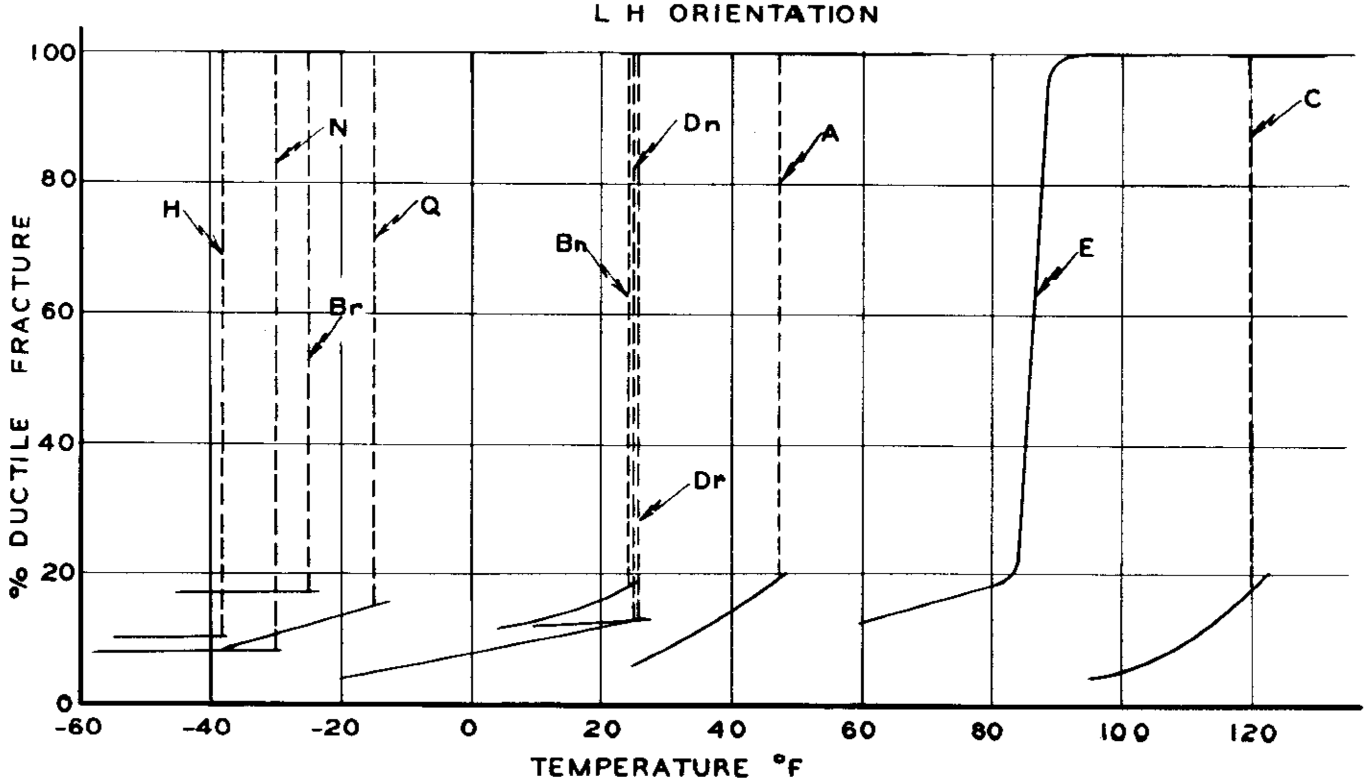

FIGURE 46

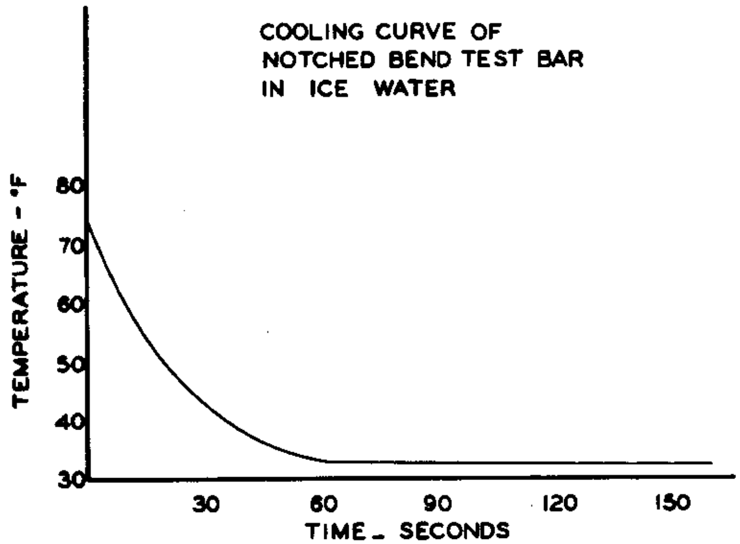

FIG. 47

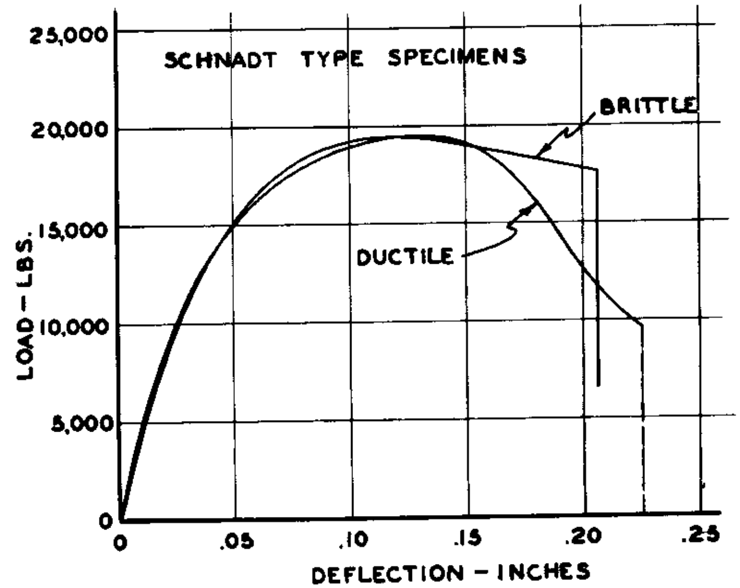

FIG. 48

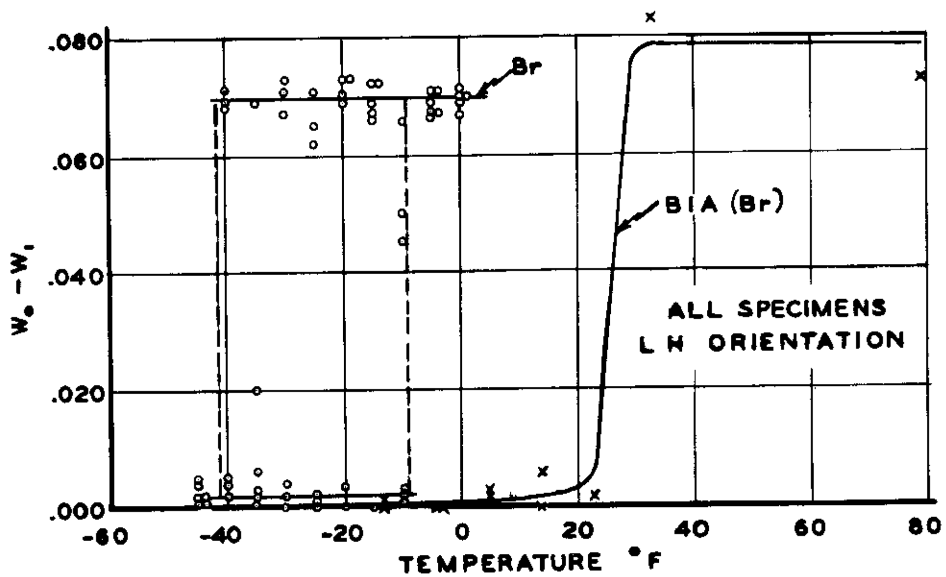

FIG. 49

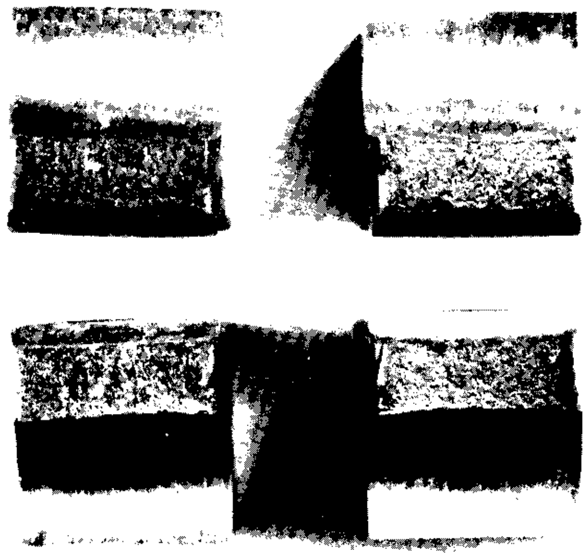

Br BlA

Figure 50

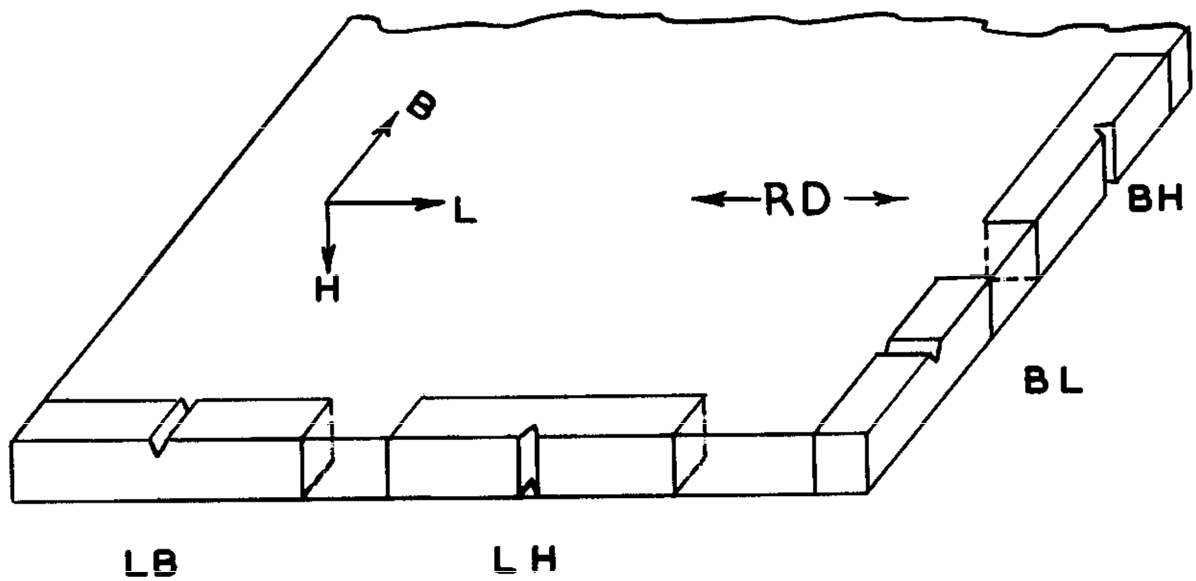

FIG. 51

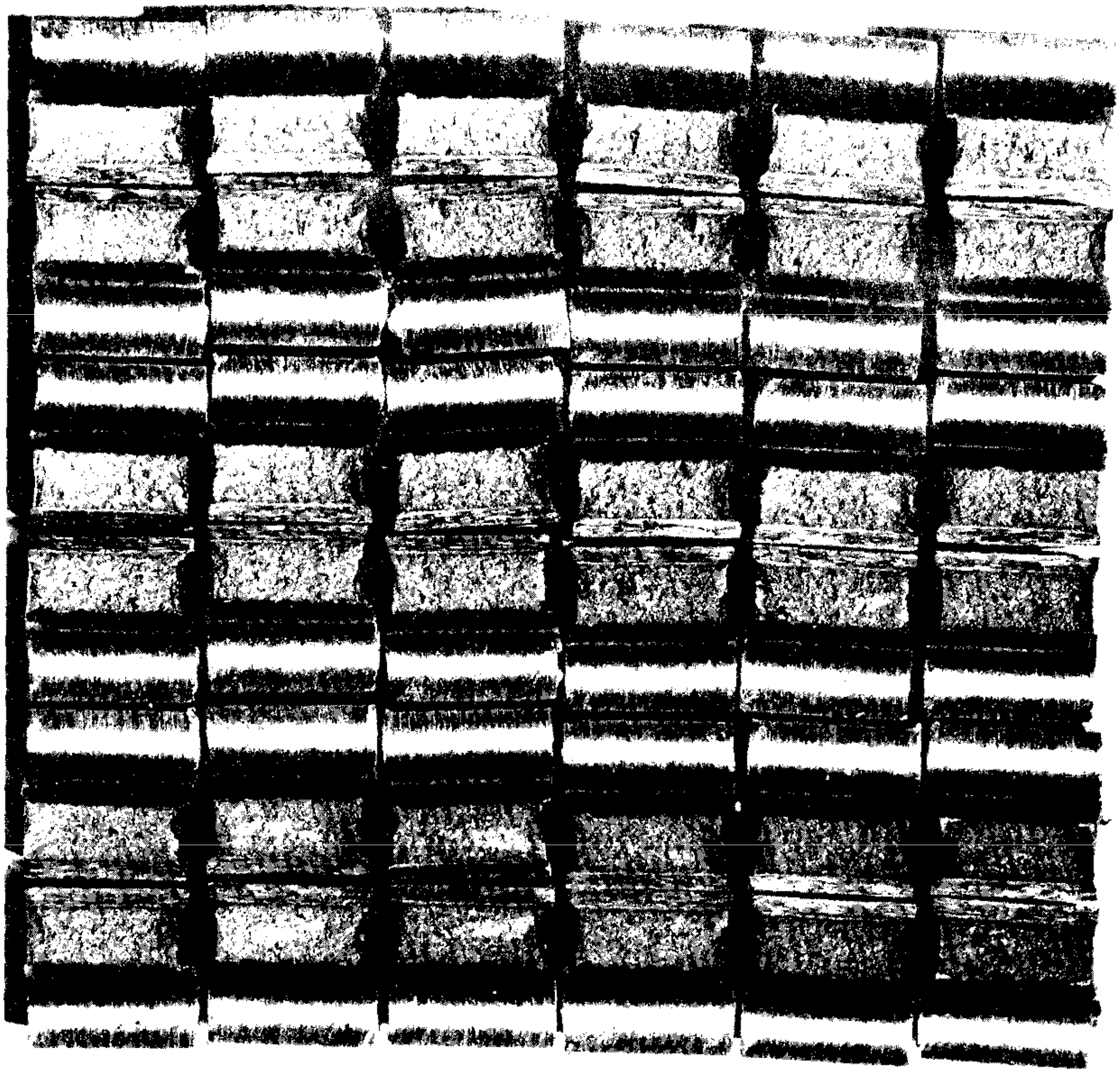

FIGURE 52-A
Steel E

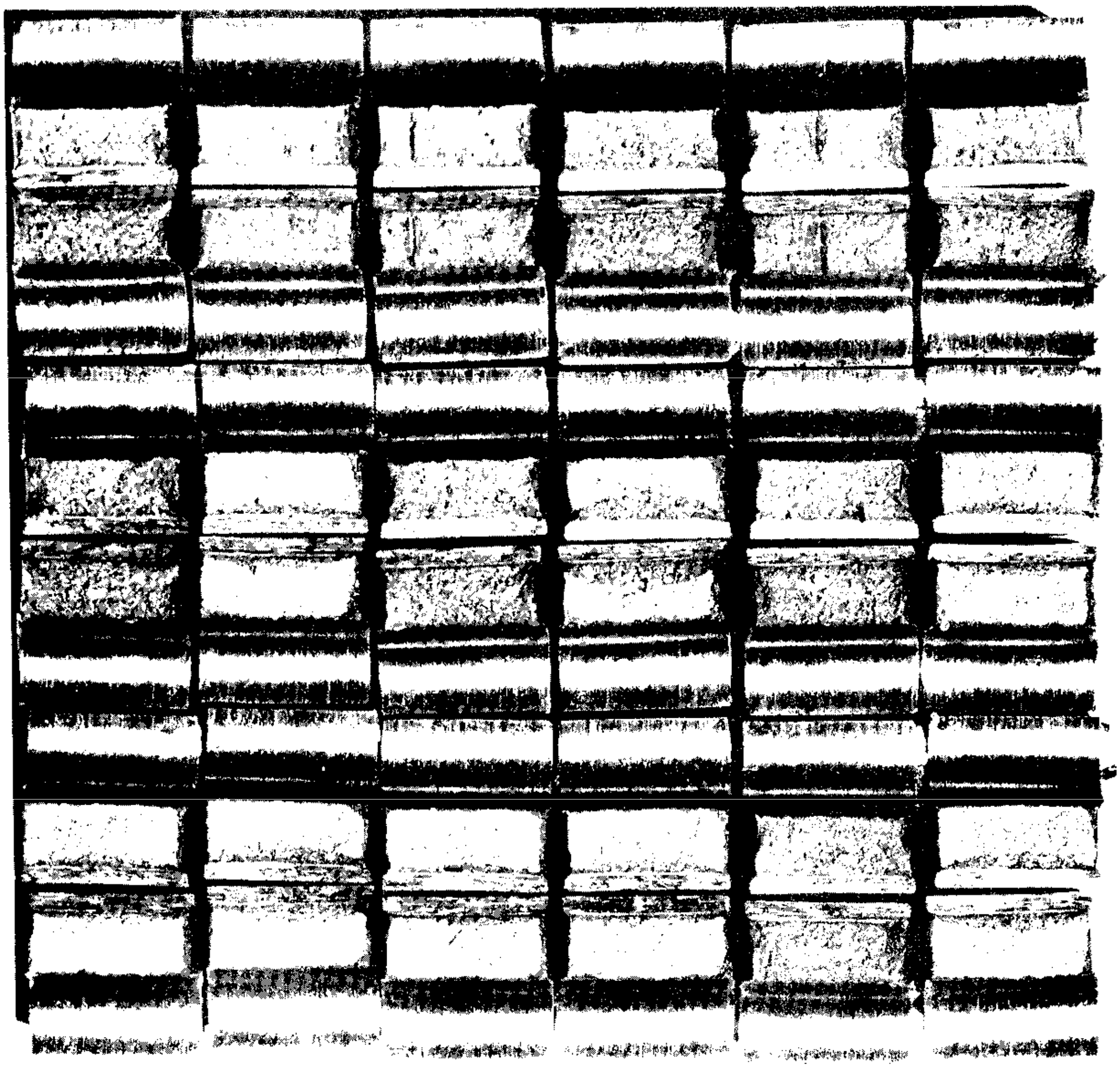

90°F

85°F

80°F

FIGURE 52-[illegible]
Steel E

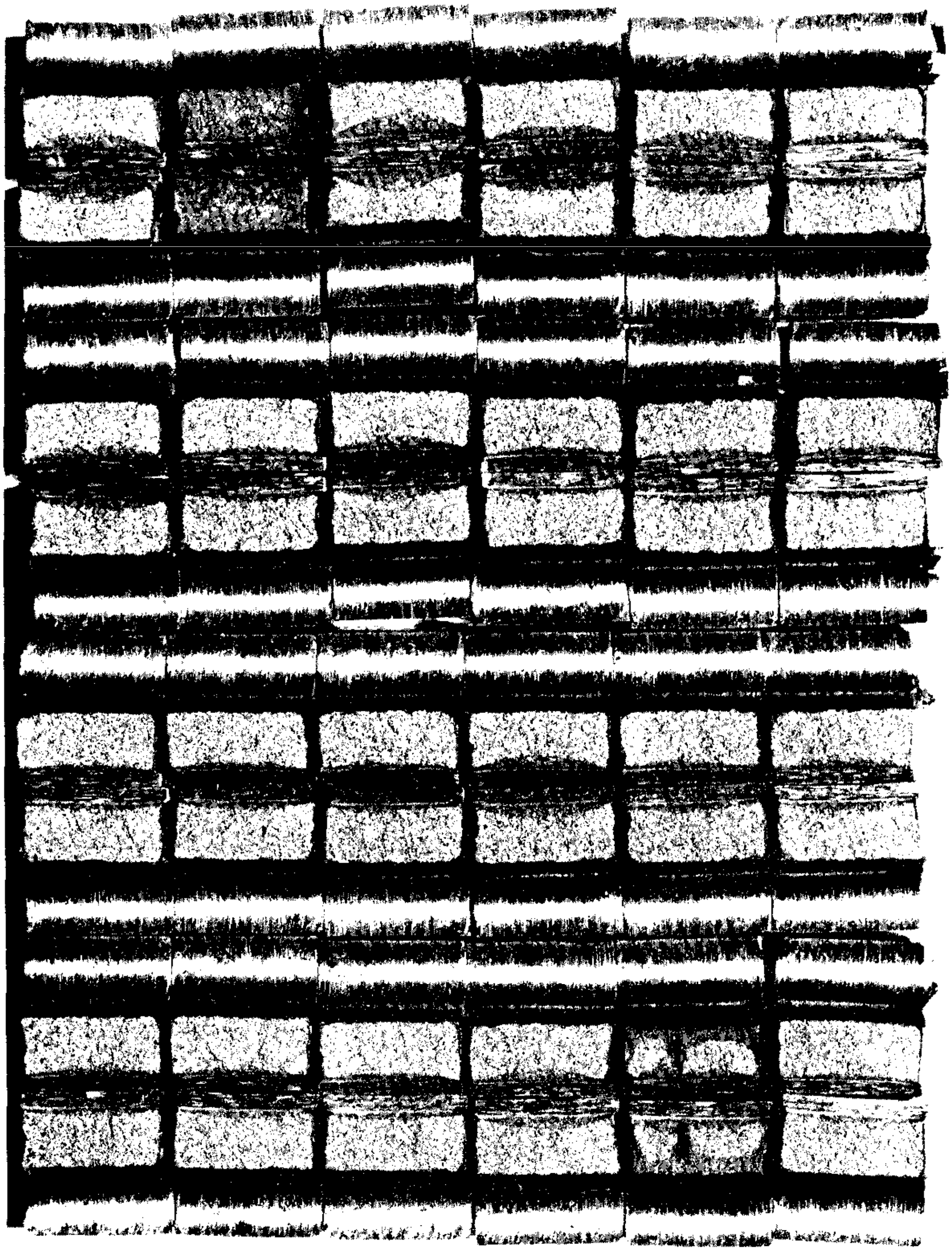

FIGURE 52-C
Steel E

0° F

-5° F

-10° F

-15° F

Figure 53A
Steel Br

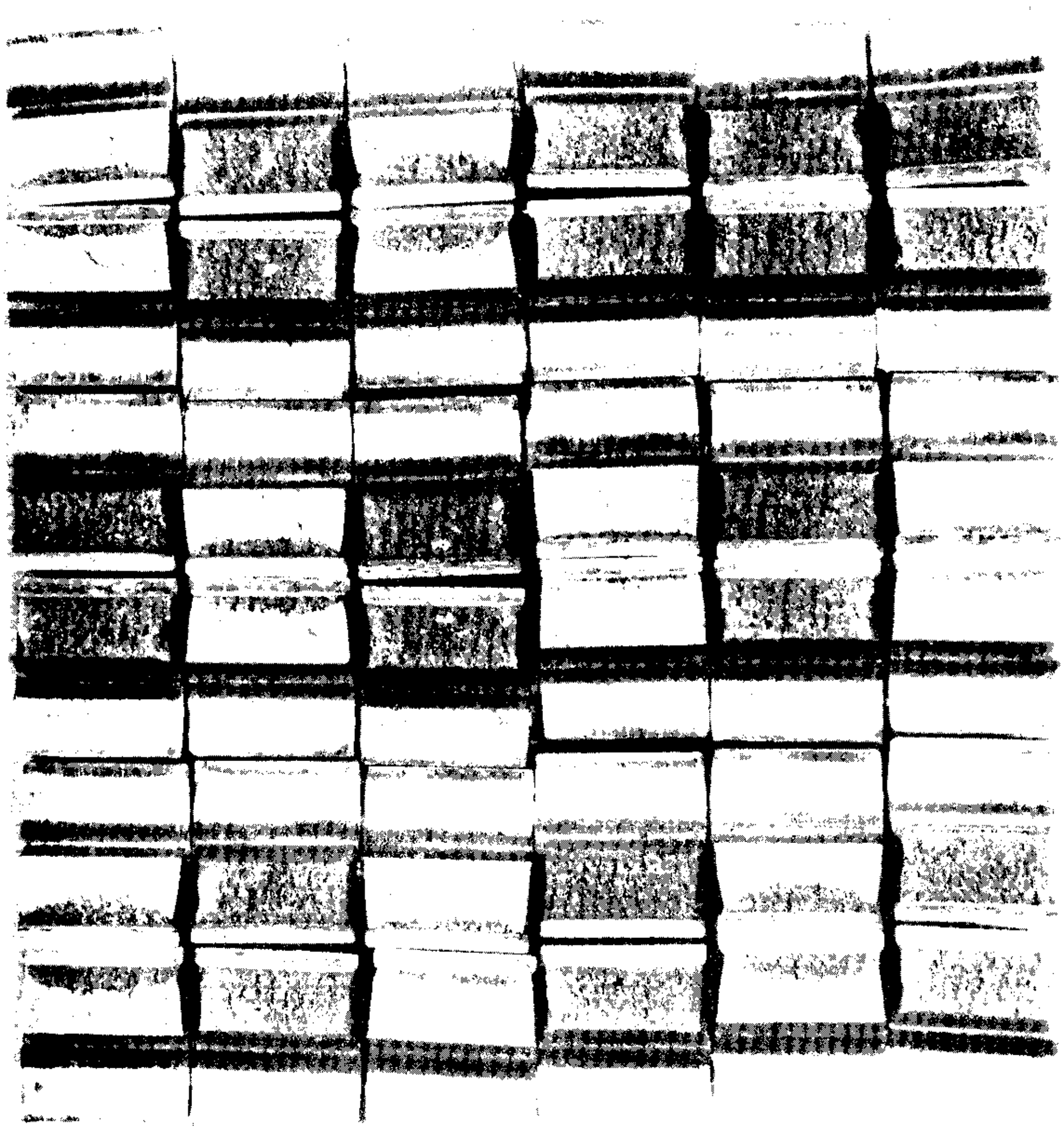

-20° F

-25° F

-30° F

Figure 53B
Steel Br

-35 ° F

-40° F

-45° F

Figure 53C-
Steel Br

TABLE A-I

Temp. °F	Spec. #	$W_o - W_1$	% Ductile Fracture	Orientation
+50	A-6	.044	100	BH
+50	A-13	.043	100	BH
+50	A-14	.035	100	BH
+41	A-3	.057	100	BH
+41	A-7	.053	100	BH
+41	A-8	.016	15	BH
+37.4	A-1	.015	15	BH
+37.4	A-11	.060	100	BH
+35.6	A-12	.011	15	BH
+23	A-5	.009	10	BH
+23	A-10	.013	10	BH
+23	A-15	.011	15	BH
+14	A-2	.002	10	BH
+14	A-4	-.002	10	BH
+14	A-9	-.001	10	BH
+37.4	Dn-8	.082	100	BH
+32	Dn-15	.075	100	BH
+32	Dn-14	.075	100	BH
+23	Dn-13	.082	100	BH
+23	Dn-12	.002	35	BH
+23	Dn-7	.077	100	BH
+14	Dn-9	.004	10	BH
+14	Dn-2	.012	15	BH
+14	Dn-1	.015	15	BH
+5	Dn-10	.007	15	BH
+5	Dn-5	.017	15	BH
-4	Dn-6	.001	10	BH
-4	Dn-4	.000	10	BH
-4	Dn-3	.005	10	BH
+41	Dr-13	.057	100	BH
+41	Dr-10	.054	100	BH
+32	Dr-8	.054	100	BH
+32	Dr-5	.012	15	BH
+32	Dr-4	.058	100	BH
+23	Dr-15	.010	35	BH
+23	Dr-9	.059	100	BH
+14	Dr-14	.010	15	BH
+14	Dr-11	.011	15	BH
+14	Dr-1	.007	15	BH
+5	Dr-12	.015	65	BH
+5	Dr-2	.005	35	BH
-4	Dr-7	.008	15	BH
-4	Dr-6	.005	15	BH
-4	Dr-3	.002	15	BH

TABLE A-I (Continued)

Temp. °F	Spec. #	$W_o - W_1$	% Ductile Fracture	Orientation
86	E-7	.063	100	BH
86	E-8	.069	100	BH
86	E-12	.073	100	BH
77	E-2	.069	100	BH
77	E-11	.051	100	BH
77	E-15	.066	100	BH
68	E-1	.034	35	BH
68	E-6	.067	100	BH
68	E-13	.069	100	BH
59	E-3	.029	35	BH
59	E-4	.026	35	BH
59	E-9	.039	15	BH
50	E-10	.028	10	BH
50	E-14	.025	10	BH
48.2	E-5	.001	15	BH
104	C-11	.043	35	BH
104	C-15	.043	50	BH
95	C-3	.024	15	BH
95	C-8	.048	100	BH
95	C-13	.036	15	BH
86	C-5	.027	15	BH
77	C-2	.029	10	BH
77	C-4	.051	100	BH
77	C-10	.052	100	BH
68	C-1	.009	10	BH
68	C-6	.020	15	BH
68	C-7	.048	100	BH
59	C-9	.025	10	BH
59	C-12	.023	15	BH
59	C-14	.015	15	BH
+14	Br-5	.058	100	BH
+14	Br-7	.050	100	BH
+14	Br-10	.053	100	BH
+5	Br-4	.052	100	BH
+5	Br-12	.055	100	BH
+5	Br-14	.065	100	BH
-4	Br-2	.054	100	BH
-4	Br-3	.057	100	BH
-4	Br-9	.062	100	BH
-13	Br-1	.058	100	BH
-13	Br-6	.060	100	BH
-22	Br-8	.062	100	BH
-22	Br-13	.014	50	BH
-31	Br-11	.059	100	BH

TABLE A-I (Continued)

Temp. °F	Spec. #	$W_o - W_1$	% Ductile Fracture	Orientation
+14	Q-4	.071	100	BH
+14	Q-9	.071	100	BH
+14	Q-12	.067	100	BH
+5	Q-1	.064	100	BH
+5	Q-2	.077	100	BH
+5	Q-13	.069	100	BH
-4	Q-5	.006	50	BH
-4	Q-10	.063	100	BH
-4	Q-11	.063	100	BH
-13	Q-3	.068	100	BH
-13	Q-7	.002	10	BH
-13	Q-15	.010	15	BH
-22	Q-6	.022	15	BH
-22	Q-8	.020	35	BH
-22	Q-14	.001	15	BH
+5	N-5	.063	100	BH
+5	N-7	.063	100	BH
+5	N-11	.063	100	BH
+5	N-14	.063	100	BH
-4	N-1	.060	100	BH
-4	N-10	.043	50	BH
-4	N-13	.060	100	BH
-13	N-3	.059	100	BH
-13	N-6	.015	15	BH
-22	N-8	.060	100	BH
-22	N-9	.010	15	BH
-22	N-15	.012	15	BH
-31	N-2	.019	10	BH
-31	N-4	.018	15	BH
-31	N-12	.014	15	BH
-4	H-3	.067	100	BH
-4	H-8	.008	35	BH
-4	H-11	.005	15	BH
-13	H-1	.062	100	BH
-13	H-9	.008	15	BH
-13	H-13	.062	100	BH
-22	H-2	.065	100	BH
-22	H-5	.066	100	BH
-22	H-15	.005	10	BH
-40	H-4	.004	35	BH
-40	H-7	.008	35	BH
-40	H-14	.009	35	BH
-49	H-6	.003	10	BH
-49	H-10	.004	10	BH
-49	H-12	.005	15	BH

TABLE A-I (Continued)

Temp. °F	Spec. #	$W_o - W_1$	% Ductile Fracture	Orientation
50	Bn-31	.070	100	LH
50	Bn-32	.064	100	LH
50	Bn-33	.071	100	LH
50	Bn-34	.066	100	LH
50	Bn-35	.068	100	LH
50	Bn-36	.061	100	LH
45	Bn-60	.061	100	LH
45	Bn-19	.063	100	LH
45	Bn-26	.059	100	LH
45	Bn-22	.069	100	LH
45	Bn-25	.064	100	LH
45	Bn-28	.065	100	LH
40	Bn-37	.065	100	LH
40	Bn-38	.060	100	LH
40	Bn-39	.055	100	LH
40	Bn-40	.058	100	LH
40	Bn-29	.071	100	LH
40	Bn-21	.064	100	LH
35	Bn-18	.010	25	LH
35	Bn-16	.071	100	LH
35	Bn-24	.063	100	LH
35	Bn-17	.068	100	LH
35	Bn-30	.061	100	LH
35	Bn-27	.066	100	LH
30	Bn-41	.069	100	LH
30	Bn-42	.001	10	LH
30	Bn-44	.066	100	LH
30	Bn-45	.022	5	LH
30	Bn-46	.000	10	LH
30	Bn-47	.009	20	LH
25	Bn-48	.062	100	LH
25	Bn-49	.002	10	LH
25	Bn-50	.008	10	LH
25	Bn-51	.009	20	LH
25	Bn-52	.058	100	LH
25	Bn-53	.005	15	LH
20	Bn-54	.075	100	LH
20	Bn-55	.006	20	LH
20	Bn-56	.008	25	LH
20	Bn-57	.071	100	LH
20	Bn-58	.006	15	LH
20	Bn-59	.005	15	LH
15	Bn-1	.004	10	LH
15	Bn-2	.008	15	LH
15	Bn-3	.002	10	LH
15	Bn-4	-.004	10	LH
15	Bn-5	.057	100	LH
15	Bn-6	.002	10	LH

TABLE A-I (Continued)

Temp. °F	Spec. #	$W_o - W_1$	% Ductile Fracture	Orientation
10	Bn-12	.002	5	LH
10	Bn-10	.001	10	LH
10	Bn-11	.000	5	LH
10	Bn-9	.011	15	LH
10	Bn-8	.007	20	LH
10	Bn-7	.004	50	LH
5	Bn-13	.002	10	LH
5	Bn-14	-.003	15	LH
5	Bn-15	.001	10	LH
70	A-1	.055	100	LH
70	A-20	.065	100	LH
70	A-14	.051	100	LH
70	A-9	.063	100	LH
65	A-53	.059	100	LH
65	A-26	.058	100	LH
65	A-49	.062	100	LH
65	A-8	.055	100	LH
65	A-38	.061	100	LH
65	A-50	.058	100	LH
60	A-12	.058	100	LH
60	A-5	.015	90	LH
60	A-29	.055	100	LH
60	A-19	.054	100	LH
60	A-4	.059	100	LH
60	A-28	.059	100	LH
55	A-30	.014	75	LH
55	A-39	.054	100	LH
55	A-16	.029	80	LH
55	A-25	.056	100	LH
55	A-18	.062	100	LH
55	A-27	.063	95	LH
50	A-54	.018	40	LH
50	A-52	.055	100	LH
50	A-33	.015	15	LH
50	A-34	.058	100	LH
50	A-48	.013	20	LH
50	A-41	.059	95	LH
45	A-55	.009	25	LH
45	A-43	.018	10	LH
45	A-57	.013	25	LH
45	A-35	.061	100	LH
45	A-46	.055	100	LH
45	A-44	.017	10	LH
40	A-59	.056	100	LH
40	A-32	.010	10	LH
40	A-40	.012	30	LH

TABLE A-I (Continued)

Temp. °F	Spec. #	$W_o - W_1$	% Ductile Fracture	Orientation
40	A-37	.061	100	LH
40	A-47	.017	40	LH
40	A-31	.009	5	LH
35	A-2	.008	0	LH
35	A-51	.008	40	LH
35	A-58	.003	25	LH
35	A-3	.009	0	LH
35	A-6	.018	0	LH
35	A-36	.012	40	LH
30	A-7	.000	0	LH
30	A-42	.008	50	LH
30	A-10	.011	0	LH
30	A-21	.007	0	LH
30	A-11	.002	20	LH
30	A-23	.009	20	LH
0	Br-19	.070	100	LH
0	Br-36	.070	100	LH
0	Br-18	.071	100	LH
0	Br-25	.069	100	LH
0	Br-34	.067	100	LH
-5	Br-9	.071	100	LH
-5	Br-13	.067	100	LH
-5	Br-26	.066	100	LH
-5	Br-27	.067	100	LH
-5	Br-8	.071	100	LH
-5	Br-12	.069	100	LH
-10	Br-15	.045	100	LH
-10	Br-17	.066	100	LH
-10	Br-32	.050	100	LH
-10	Br-54	.003	10	LH
-10	Br-30	.001	30	LH
-10	Br-3	.002	15	LH
-15	Br-23	.069	100	LH
-15	Br-21	.072	100	LH
-15	Br-22	.072	100	LH
-15	Br-52	.067	100	LH
-15	Br-48	.000	20	LH
-15	Br-1	.066	100	LH
-20	Br-47	.070	100	LH
-20	Br-59	.004	40	LH
-20	Br-53	.000	15	LH
-20	Br-58	.073	100	LH
-20	Br-39	.069	100	LH
-20	Br-56	.073	100	LH
-25	Br-38	.062	100	LH
-25	Br-5	.000	5	LH

TABLE A-I (Continued)

Temp. °F	Spec. #	$W_o - W_1$	% Ductile Fracture	Orientation
-25	Br-24	.001	10	LH
-25	Br-20	.065	100	LH
-25	Br-10	.071	100	LH
-25	Br-60	.002	20	LH
-30	Br-29	.073	100	LH
-30	Br-33	.067	100	LH
-30	Br-4	.000	30	LH
-30	Br-28	.004	30	LH
-30	Br-6	.002	10	LH
-30	Br-43	.071	100	LH
-35	Br-37	.003	100	LH
-35	Br-2	.020	60	LH
-35	Br-55	.002	25	LH
-35	Br-50	.066	100	LH
-35	Br-41	.001	15	LH
-35	Br-31	.069	100	LH
-40	Br-14	.068	100	LH
-40	Br-35	.069	100	LH
-40	Br-40	.002	10	LH
-40	Br-51	.005	20	LH
-40	Br-42	.004	25	LH
-40	Br-49	.071	100	LH
-45	Br-44	.001	20	LH
-45	Br-7	.005	25	LH
-45	Br-16	.001	5	LH
-45	Br-6	.002	10	LH
-45	Br-57	.004	20	LH
-45	Br-45	.002	10	LH
105	E-60	.065	100	LH
105	E-25	.061	100	LH
105	E-58	.058	100	LH
105	E-7	.057	100	LH
105	E-27	.052	100	LH
105	E-29	.065	100	LH
100	E-28	.062	100	LH
100	E-23	.066	100	LH
100	E-22	.065	100	LH
100	E-24	.057	100	LH
100	E-17	.065	100	LH
100	E-5	.073	100	LH
95	E-54	.055	100	LH
95	E-8	.054	100	LH
95	E-9	.062	100	LH
95	E-59	.077	85	LH
95	E-56	.068	85	LH
95	E-21	.057	100	LH

TABLE A-I (Continued)

Temp. °F	Spec. #	$W_o - W_1$	% Ductile Fracture	Orientation
90	E-26	.080	100	LH
90	E-36	.072	100	LH
90	E-37	.068	100	LH
90	E-51	.083	100	LH
90	E-43	.074	100	LH
90	E-57	.071	100	LH
85	E-53	.062	100	LH
85	E-33	.034	35	LH
85	E-32	.065	100	LH
85	E-46	.032	35	LH
85	E-44	.031	50	LH
85	E-31	.060	100	LH
80	E-45	.077	100	LH
80	E-20	.031	15	LH
80	E-39	.027	15	LH
80	E-40	.022	10	LH
80	E-1	.031	15	LH
80	E-16	.030	10	LH
75	E-30	.030	35	LH
75	E-55	.025	15	LH
75	E-2	.030	15	LH
75	E-34	.071	100	LH
75	E-38	.035	15	LH
75	E-14	.031	35	LH
70	E-15	.023	15	LH
70	E-4	.018	10	LH
70	E-42	.008	15	LH
70	E-52	.017	10	LH
70	E-3	.018	10	LH
70	E-18	.012	10	LH
65	E-11	.011	10	LH
65	E-47	.020	10	LH
65	E-19	.013	15	LH
65	E-12	.012	10	LH
65	E-6	.013	10	LH
65	E-50	.019	10	LH
60	E-13	.010	10	LH
60	E-48	.009	10	LH
60	E-35	.058	50	LH
60	E-49	.012	10	LH
60	E-41	.011	10	LH
60	E-10	.016	10	LH

TABLE A-I (Continued)

Temp. °F	Spec. #	$w_o - w_1$	% Ductile Fracture	Orientation
55	Dr-27	.042	100	LH
55	Dr-20	.031	100	LH
55	Dr-14	.040	100	LH
55	Dr-8	.054	100	LH
55	Dr-9	.040	100	LH
50	Dr-7	.054	100	LH
50	Dr-58	.056	100	LH
50	Dr-19	.061	100	LH
50	Dr-13	.014	25	LH
50	Dr-32	.015	55	LH
50	Dr-1	.059	100	LH
45	Dr-46	.065	100	LH
45	Dr-34	.056	100	LH
45	Dr-40	.074	100	LH
45	Dr-17	.065	100	LH
45	Dr-55	.065	100	LH
45	Dr-51	.066	100	LH
40	Dr-30	.058	100	LH
40	Dr-22	.005	10	LH
40	Dr-10	.057	100	LH
40	Dr-24	.061	100	LH
40	Dr-57	.065	100	LH
40	Dr-12	.017	70	LH
35	Dr-47	.006	10	LH
35	Dr-54	.062	100	LH
35	Dr-36	.025	60	LH
35	Dr-44	.014	10	LH
35	Dr-42	.018	10	LH
35	Dr-35	.017	40	LH
30	Dr-26	.000	10	LH
30	Dr-37	.059	100	LH
30	Dr-45	.002	10	LH
30	Dr-38	.003	15	LH
30	Dr-53	.053	100	LH
30	Dr-31	.057	100	LH
25	Dr-41	.061	100	LH
25	Dr-59	.065	100	LH
25	Dr-39	.007	25	LH
25	Dr-60	.010	60	LH
25	Dr-52	.006	30	LH
25	Dr-48	.005	50	LH
20	Dr-25	.005	20	LH
20	Dr-18	-.002	10	LH
20	Dr-28	.052	100	LH

TABLE A-I (Continued)

Temp. °F	Spec. #	$w_o - w_1$	% Ductile Fracture	Orientation
20	Dr-6	.001	15	LH
20	Dr-15	.003	10	LH
20	Dr-3	.011	50	LH
15	Dr-50	.071	100	LH
15	Dr-29	.000	5	LH
15	Dr-4	.002	10	LH
15	Dr-33	.002	5	LH
15	Dr-5	.009	10	LH
15	Dr-49	.004	15	LH
10	Dr-43	.019	30	LH
10	Dr-11	.014	70	LH
10	Dr-16	.005	10	LH
10	Dr-2	.001	20	LH
10	Dr-21	.004	10	LH
10	Dr-23	.056	100	LH
+5	Q-5	.052	100	LH
+5	Q-4	.051	100	LH
+5	Q-8	.065	100	LH
+5	Q-7	.060	100	LH
+5	Q-6	.060	100	LH
+5	Q-9	.059	100	LH
0	Q-10	.062	100	LH
0	Q-12	.016	15	LH
0	Q-11	.061	100	LH
0	Q-13	.027	30	LH
0	Q-17	.004	10	LH
0	Q-14	.060	100	LH
-5	Q-1	.016	50	LH
-5	Q-3	.063	100	LH
-5	Q-2	.023	15	LH
-5	Q-16	.034	60	LH
-5	Q-19	.011	30	LH
-5	Q-18	.052	100	LH
-10	Q-20	.009	5	LH
-10	Q-22	.040	80	LH
-10	Q-23	.052	100	LH
-10	Q-24	.017	5	LH
-10	Q-25	.062	100	LH
-10	Q-32	.058	100	LH
-15	Q-26	.000	30	LH
-15	Q-27	.028	70	LH
-15	Q-29	.011	15	LH
-15	Q-28	.014	15	LH
-15	Q-31	.006	25	LH
-15	Q-30	.014	5	LH

TABLE A-I (Continued)

Temp. °F	Spec. #	$w_o - w_1$	% Ductile Fracture	Orientation
-20	Q-15	.004	2	LH
-20	Q-36	.012	5	LH
-20	Q-35	.011	10	LH
-20	Q-41	.061	100	LH
-20	Q-40	.019	15	LH
-20	Q-39	.010	5	LH
-25	Q-34	.028	20	LH
-25	Q-43	-.003	5	LH
-25	Q-46	.011	45	LH
-25	Q-37	.020	25	LH
-25	Q-45	.006	25	LH
-25	Q-42	.020	15	LH
-30	Q-47	.012	25	LH
-30	Q-38	.002	10	LH
-30	Q-33	.029	25	LH
-30	Q-49	.008	10	LH
-30	Q-53	.059	100	LH
-30	Q-52	-.003	2	LH
-35	Q-50	.002	10	LH
-35	Q-51	.029	60	LH
-35	Q-54	.036	20	LH
-35	Q-58	.006	5	LH
-35	Q-56	.021	15	LH
-35	Q-55	-.003	2	LH
-40	Q-48	.014	15	LH
-40	Q-44	.006	0	LH
-40	Q-57	.000	2	LH
-40	Q-59	.002	5	LH
-40	Q-60	.004	2	LH
-15	H-9	.059	100	LH
-15	H-12	.064	100	LH
-15	H-38	.063	100	LH
-15	H-13	.065	100	LH
-20	H-37	.075	100	LH
-20	H-23	.019	70	LH
-20	H-24	.061	100	LH
-20	H-4	.025	90	LH
-25	H-40	.061	100	LH
-25	H-25	.002	5	LH
-25	H-36	.063	100	LH
-25	H-26	.071	100	LH
-30	H-42	.061	100	LH
-30	H-30	.066	100	LH
-30	H-11	.029	90	LH
-30	H-6	.018	50	LH

TABLE A-I (Continued)

Temp. ^oF	Spec. #	$w_o - w_1$	% Ductile Fracture	Orientation
-35	H-17	.005	5	LH
-35	H-1	.003	10	LH
-35	H-22	.066	100	LH
-35	H-35	.029	85	LH
-40	H-34	.054	100	LH
-40	H-3	.057	100	LH
-40	H-18	.002	30	LH
-40	H-39	.021	40	LH
-45	H-32	.003	10	LH
-45	H-27	.006	20	LH
-45	H-31	.005	20	LH
-45	H-16	.012	25	LH
-50	H-28	.003	0	LH
-50	H-33	.001	10	LH
-50	H-21	.072	100	LH
-50	H-19	.007	15	LH
-50	H-29	.004	5	LH
-55	H-14	.010	30	LH
-55	H-2	.007	0	LH
-55	H-5	.008	20	LH
-55	H-8	.006	15	LH
+130	C-43	.045	100	LH
+130	C-49	.044	100	LH
+130	C-3	.051	100	LH
+130	C-38	.051	100	LH
+130	C-42	.046	97	LH
+130	C-57	.050	100	LH
+125	C-37	.048	85	LH
+125	C-48	.039	55	LH
+125	C-60	.049	70	LH
+125	C-50	.040	25	LH
+125	C-24	.043	80	LH
+125	C-9	.051	50	LH
+120	C-32	.051	50	LH
+120	C-52	.048	60	LH
+120	C-23	.055	90	LH
+120	C-46	.030	20	LH
+120	C-34	.048	30	LH
+120	C-22	.044	50	LH
+115	C-4	.053	100	LH
+115	C-8	.028	20	LH
+115	C-33	.017	10	LH
+115	C-28	.032	20	LH
+115	C-35	.026	30	LH
+115	C-11	.053	75	LH

TABLE A-I (Continued)

Temp. °F	Spec. #	$w_o - w_1$	% Ductile Fracture	Orientation
+110	C-12	.032	40	LH
+110	C-30	.031	30	LH
+110	C-17	.030	40	LH
+110	C-47	.032	40	LH
+110	C-55	.035	10	LH
+110	C-2	.026	10	LH
+105	C-31	.054	60	LH
+105	C-40	.017	10	LH
+105	C-10	.019	5	LH
+105	C-15	.029	20	LH
+105	C-14	.027	20	LH
+105	C-6	.022	20	LH
+100	C-36	.029	5	LH
+100	C-41	.022	5	LH
+100	C-18	.031	5	LH
+100	C-19	.030	5	LH
+100	C-39	.030	10	LH
+100	C-53	.028	15	LH
+ 95	C-16	.025	5	LH
+ 95	C-7	.026	5	LH
+ 95	C-1	.030	5	LH
+ 35	C-27	.004	0	LH
+ 35	C-25	.003	0	LH
+40	Dn-40	.070	100	LH
+40	Dn-26	.070	100	LH
+40	Dn-7	.023	50	LH
+40	Dn-41	.073	100	LH
+40	Dn-50	.066	100	LH
+35	Dn-16	.067	100	LH
+35	Dn-42	.067	100	LH
+35	Dn-36	.070	100	LH
+35	Dn-60	.067	100	LH
+30	Dn-37	.067	100	LH
+30	Dn-52	.068	100	LH
+30	Dn-3	.075	100	LH
+30	Dn-47	.065	100	LH
+25	Dn-20	.069	100	LH
+25	Dn-22	.003	15	LH
+20	Dn-45	.066	100	LH
+20	Dn-24	.014	10	LH
+20	Dn-44	.017	20	LH
+20	Dn-27	.071	100	LH
+20	Dn-51	.070	100	LH
+15	Dn-11	.010	5	LH
+15	Dn-21	.067	100	LH
+15	Dn-13	.072	100	LH

TABLE A-I (Continued)

Temp. °F	Spec. #	$w_o - w_1$	% Ductile Fracture	Orientation
+15	Dn-28	.003	100	LH
+15	Dn-14	.008	20	LH
+15	Dn-58	.057	100	LH
+10	Dn-59	.010	3	LH
+10	Dn-4	.010	5	LH
+10	Dn-30	.012	5	LH
+10	Dn-23	.004	5	LH
+10	Dn-57	.082	100	LH
+10	Dn-34	.009	20	LH
+ 5	Dn-53	.005	5	LH
+ 5	Dn-38	.012	30	LH
+ 5	Dn-33	.021	50	LH
+ 5	Dn-35	.000	5	LH
+ 5	Dn-12	.005	5	LH
0	Dn-56	.010	20	LH
0	Dn-2	.002	5	LH
0	Dn-17	.000	5	LH
0	Dn-48	.003	5	LH
0	Dn-1	.006	2	LH
-10	Dn-54	.000	5	LH
-10	Dn-39	.004	5	LH
-10	Dn-5	-.001	0	LH
-10	Dn-25	-.001	1	LH
-10	Dn-8	.003	1	LH
-10	Dn-32	-.002	1	LH
-15	Dn-43	-.001	0	LH
-15	Dn-55	.002	15	LH
-15	Dn-15	-.003	2	LH
-15	Dn-29	.001	2	LH
-15	Dn-39	-.001	0	LH
-15	Dn-46	.001	1	LH
-20	Dn-9	.001	0	LH
-20	Dn-18	.003	0	LH
-20	Dn-6	.002	0	LH
-20	Dn-10	.007	0	LH
-20	Dn-49	.000	0	LH
-20	Dn-19	.001	0	LH